



Jane Yura
Vice President
Asset & Risk Management
Gas Operations

6111 Bollinger Canyon
4th Floor
San Ramon, CA 94583

925 244-3398
JKY1@pge.com

January 17, 2014

Elizaveta Malashenko
Deputy Director
Office of Utility Safety and Reliability
Safety and Enforcement Division
California Public Utilities Commission

Re: Update - Oakland Incident of December 10, 2013

Dear Ms. Malashenko,

This letter is to provide an update on the incident that occurred on December 10, 2013, near [Redacted] in Oakland. PG&E provided the first update regarding this incident on December 20, 2013. PG&E is now providing a second update to summarize Exponent, Inc.'s final report findings and analysis of the incident, as well as PG&E's next steps. The report, "[Redacted] (Oakland) Incident Analysis," includes an Executive Summary and is provided as an attachment to this letter.

Exponent's comprehensive investigation included inspection of the leak site, historical review of PG&E's construction documents, a fire cause and origin study, metallurgical analysis, geotechnical analysis, analysis of other leak locations within the immediate area, and finite element-based stress analysis of the effect of ground movement on the subject elbow and associated piping. The report concludes that the most likely root cause of the elbow fracture was from stresses that developed over time due to creep along the Hayward Fault.¹ The report also confirms the findings described in our December 20, 2013 letter for metallurgical analysis, finite element modeling, and potential sources of ignition. A summary of the report's conclusions are provided below.

- Leaking natural gas was ignited on the ground/street surface directly above the broken elbow most likely by passing traffic or a transient source such as a discarded cigarette.
- The subject elbow fractured in a brittle manner, and no evidence of progressive cracking, such as fatigue or stress corrosion cracking (SCC) was observed. There were no manufacturing defects, mechanical damage, or wall thinning due to corrosion that contributed to the break. The leak site

¹ Creep is a slow relative movement of land along a fault zone. In this case, it is measured in millimeters per year and can take many years before signs of creep become apparent. Road resurfacing and sidewalk repairs can easily obscure the signs of creep, making it not easily detectable.

is located within the Hayward Fault Zone, and also lies within a narrower zone containing an actively creeping fault trace. The leak site also lies within an ancient landslide area. Ground-movement shear is the likely cause of the stresses that resulted in the elbow rupture. Other possible ground movement mechanisms - recent landslide movement, seismic activity, and settlement - were evaluated and determined to be unlikely to have significantly contributed to the elbow rupture. Exponent also determined that stresses from heavy equipment road-surface loading as well as the apparent 2003 sewer-line rehabilitation were unlikely contributors.

- Exponent's stress analysis indicates that local stresses likely persist in portions of the remaining pipe system in the area. Exponent recommends those facilities be replaced to relieve the current stresses.

Following the December 10, 2013 release, PG&E conducted a special leak survey and corresponding repair excavations in the area of [Redacted]

[Redacted] Exponent observed fourteen excavations in which twelve leaks were detected and repaired. These included all of the Grade 1, 2+, and 2 leaks identified during the survey, and also several Grade 3 leaks. Exponent observed no evidence that any of the leaks resulted from ground movement. Exponent observed no indications of similar external load damage to the pipes exposed in the excavations. PG&E has completed leak repairs of the Grade 1 leak and seven Grade 2+ and Grade 2 leaks identified from the special leak survey and continues to monitor the Grade 3 leaks in accordance with our leak survey program.

Based on the results of the comprehensive failure analysis, PG&E plans to take additional actions in response to this event:

1. PG&E will modify the piping at the original leak location including existing elbows that change the direction of the pipe from [Redacted] to [Redacted]. Although the failed components were removed, the remaining pipe at this location could still be under load as a result of fault creep.
2. In the neighborhood and vicinity of the leak location, PG&E will perform additional studies to determine if any other pipe configurations in the vicinity of the Hayward Fault creep trace could be vulnerable to earth displacement loads. Piping configurations to be evaluated will be those that involve pipe directional changes (e.g., elbows, junctions, and tees) that occur within the fault creep zone.
3. PG&E also recognizes the broader implication of the root cause results. PG&E has an extensive network of distribution piping and as a result, some pipelines are unavoidably in the vicinity of earthquake faults. To address the broader implications, PG&E plans to incorporate the seismic creep threat into its Distribution Integrity Management Program.

Elizaveta Malashenko
January 17, 2014
Page 3

Please let me know if you have any questions or require further information.

Sincerely,

A handwritten signature in black ink, appearing to read "Jane Yura".

Jane Yura
Vice President, Risk and Asset Management

Cc: Paul Clanon, CPUC
General Jack Hagan, CPUC

Redacted, PG&E
Laura Doll, PG&E
Bill Gibson, PG&E

Attachment

Failure Analysis Associates

Exponent[®]

Redacted

(Oakland)

Incident Analysis



Redacted

(Oakland)

Incident Analysis

Prepared for

Sumeet Singh
Pacific Gas and Electric Company
6111 Bollinger Canyon Road
San Ramon, CA 94583

Prepared by

Exponent
149 Commonwealth Drive
Menlo Park, CA 94025

January 2014

© Exponent, Inc.

Doc. no. 1308766.000 - 7422

Contents

	<u>Page</u>
Limitations	iii
Executive Summary	iv
Background and Site Inspection	1
Gas Distribution Mains, Sewer Line, and Water Line Construction	4
Ignition Source Analysis	11
Metallurgical Failure Analysis	14
Visual Examination	14
Fractography	16
Metallographic Examination	22
Mechanical Testing	23
Chemical Analysis	24
Metallurgical Discussion	25
Geotechnical Analysis	26
Physical Setting	26
Summary of Ground Movement Mechanisms Evaluated	26
Fault-Creep Ground Deformation	27
Recent Seismic Activity	40
Non-Seismic Ground Settlement	40
Landslide Movement	41
Stress Analysis	44
Gravitational Loading	47
Ground Movement Shearing	49
Post-Failure Repair	60
Stress Analysis Discussion	61
Post-Survey Observation of Repair Excavations	63
Threat Category Assessment	65
Conclusions	67

Limitations

The scope of services performed during this investigation may not adequately address the needs of other users of this report, and any re-use of this report or its findings, conclusions, or recommendations presented herein is at the sole risk of the user. The opinions and comments formulated during this assessment are based on observations and information available at the time of the investigation. No guarantee or warranty as to future life or performance of any reviewed condition is expressed or implied.

Exponent has no direct knowledge of, and offers no warranty regarding the condition of concealed construction or subsurface conditions beyond what was exposed during our investigation. Comments regarding concealed construction or subsurface conditions are professional opinions, derived in accordance with current standards of professional practice based on our geologic and engineering experience and judgment.

The findings presented herein are made to a reasonable degree of scientific and engineering certainty. We have made every effort to accurately and completely investigate all areas of concern identified during our investigation. If new data becomes available or there are perceived omissions or misstatements in this report regarding any aspect of those conditions, we ask that they be brought to our attention as soon as possible so that we have the opportunity to fully address them.

Executive Summary

Pacific Gas and Electric (PG&E) has retained Exponent Failure Analysis Associates (Exponent) to conduct a failure analysis investigation of an elbow that fractured as part of a four-inch natural gas distribution line on December 10, 2013 near the intersection of [Redacted] and [Redacted] in Oakland, California. Our investigation to-date has included inspection of the leak site, review of PG&E's historical construction documents, a fire cause and origin study, metallurgical analysis, geotechnical analysis, analysis of other leak locations within the immediate area, and finite element-based stress analyses of ground movement and stresses on the subject elbow and associated piping.

Exponent's analyses indicate that the most likely root cause of the subject elbow fracture was from stresses that developed over time due to creep along the Hayward Fault.

The subject elbow was part of a 1946 installation of four-inch steel pipe that runs along [Redacted] [Redacted]. In 1965, a tee to a three-inch diameter steel pipe main that extends along [Redacted] [Redacted] was added just upstream of the subject elbow. Additional work was conducted in the area in 1987 when a four-inch diameter plastic line was installed along [Redacted] downstream of the subject elbow. As part of this installation a three-inch tee and a steel riser section were placed just downstream of the subject elbow. Our review of the as-built construction drawings shows that they are consistent with the features observed in the ground. Other utilities were also observed to be in close proximity to the fractured elbow: a sanitary sewer line that runs parallel to [Redacted] and a water main lateral that runs approximately transverse to [Redacted] [Redacted].

After the subject elbow fracture, natural gas was ignited on the ground/street surface. Ignition from the various utilities in the area was determined to be unlikely. The most likely cause(s) of ignition were from a passing automobile, or by transient sources, such as a discarded cigarette.

Metallurgical analysis definitively determined that the subject elbow fractured because it was subjected to stresses higher than its tensile strength. The elbow fractured in a brittle manner, and no evidence of progressive cracking, such as fatigue or stress corrosion cracking (SCC), was observed. There were no manufacturing defects, mechanical damage, or wall thinning due to corrosion that contributed to the break. The pipe elbow (and adjacent four-inch, 1946 steel pipe) met the pertinent standards for tensile properties and chemistry.

The leak site is located within the Hayward Fault Zone, and also lies within a narrower zone in which the actively creeping fault trace has been mapped by the USGS. The leak site also lies within a mapped ancient landslide. Ground-movement shear, caused by creep along this section of the right-lateral strike-slip Hayward Fault, is the likely cause of the stresses that resulted in the elbow rupture. Other ground movement mechanisms - recent landslide movement, seismic activity, and settlement - were evaluated and determined to be unlikely to have significantly contributed to the elbow rupture.

Finite element analysis indicated that the subject elbow likely fractured from stresses accumulated from creep along the Hayward Fault. Finite element analysis also indicated that

landslide shearing also produced stresses in the pipe network that are consistent with the failure location and failure mode; however, there was no observed or documented evidence of recent landsliding in the vicinity of the pipe failure. Ground settlement and loading from heavy equipment on the road surface have been determined to be unlikely as potential contributors to the break because they do not produce stresses that are consistent with the failure location and failure mode. Installation of the sanitary sewer line has been determined to be unlikely as a potential contributor to the break because the line was installed in 2003, approximately ten years prior to the incident, and thus is unlikely to significantly affect the stresses at the time of the rupture.

After the failure, the connection between the [Redacted] pipe and the [Redacted] pipe remains intact. Exponent's stress analysis indicates that local stresses likely remain in the existing configuration. As more fault creep occurs in the future, these stresses are expected to increase. Exponent recommends the current connection be replaced to relieve the current stresses.

Following the December 10, 2013 release, PG&E conducted leak surveys and corresponding repair excavations along gas mains within the general vicinity. Exponent observed fourteen excavations in which twelve leaks were detected and repaired. These included all of the Grade 1, 2+, and 2 leaks identified during the survey, and also several Grade 3 leaks. None of the leaks was caused by ground movement. Nine of the leaks were caused by local corrosion of steel piping, one was a pinhole leak in a weld, two occurred at loose caps on plastic pipes, and one occurred in a cracked plastic fitting.

This Executive Summary does not contain all of Exponent's technical evaluations, analyses, conclusions, and recommendations. Hence, the main body of this report is at all times the controlling document.

Background and Site Inspection

On December 10, 2013, a 4-inch nominal diameter underground natural gas distribution line owned by Pacific Gas and Electric Company (PG&E) fractured and caused a natural gas release in Oakland, California. The fractured pipe was located near the intersection of [Redacted] and [Redacted]. The area of the release is shown in Figure 1.

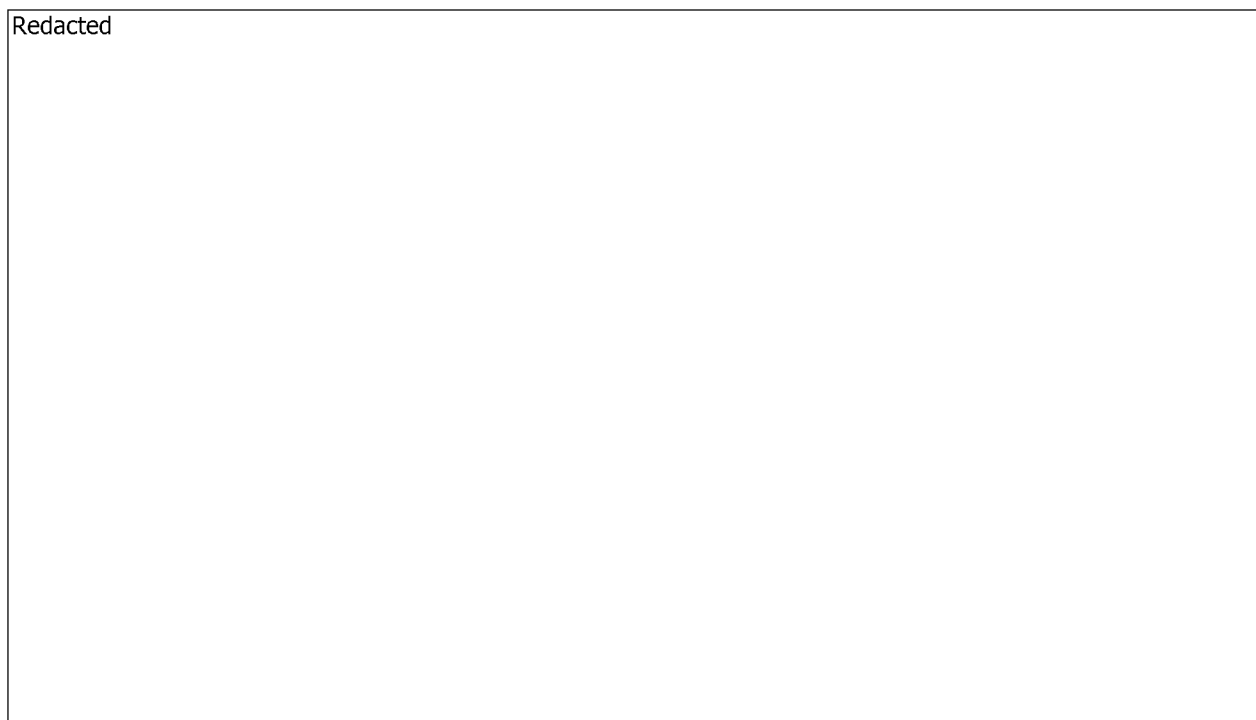


Figure 1. Area of the leak (satellite image from Google Maps).

The released gas was ignited and resulted in a gas-fueled fire, which is shown in Figure 2. The fire was first reported to PG&E at approximately 8:39 a.m. and at 8:44 a.m. PG&E personnel arrived on site. The responding fire crews allowed the fire to burn in order to prevent an explosive accumulation of gas from forming. The fire continued to burn until after the upstream flow of gas was shut off at approximately 11:35 a.m. by cutting, capping, and welding the 4-inch main in three locations. No injuries or fatalities occurred and the total damages were reported to be less than \$50,000.



Figure 2. Image of the fire resulting from gas release. Source: PG&E

An excavation of the area of the gas release site, shown in Figure 3, revealed steel natural gas distribution mains, a water main lateral, and a sanitary sewer line in the immediate vicinity. Upon visual inspection, it was determined that the source of the gas release was a fractured elbow. A portion of the fractured elbow, while still covered with pipe wrap, is shown partially protruding from the soil in Figure 3. The continuation of the 4-inch gas main, the adjacent water pipe, and the sanitary sewer main are also shown. The fractured elbow is shown prior to removal in Figure 4. The flanged tee and 3-inch pipe shown in Figure 4 were not removed from the ground. Following Exponent's site inspection, the fractured elbow and several adjacent pipeline features were removed and retained by Exponent for laboratory inspection. The gas main features that were removed and their respective installation dates are shown in Figure 5. The features in Figure 5 are shown as they would have been seen if the viewer were facing approximately northwest.

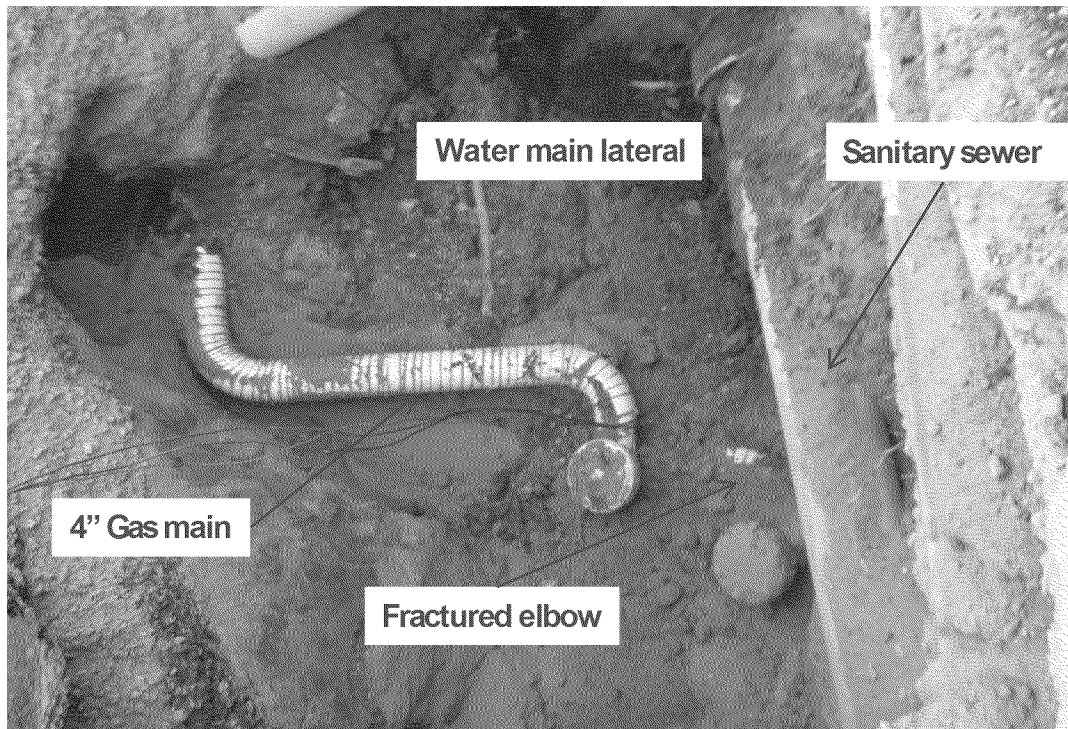


Figure 3. Excavated area of the gas release.

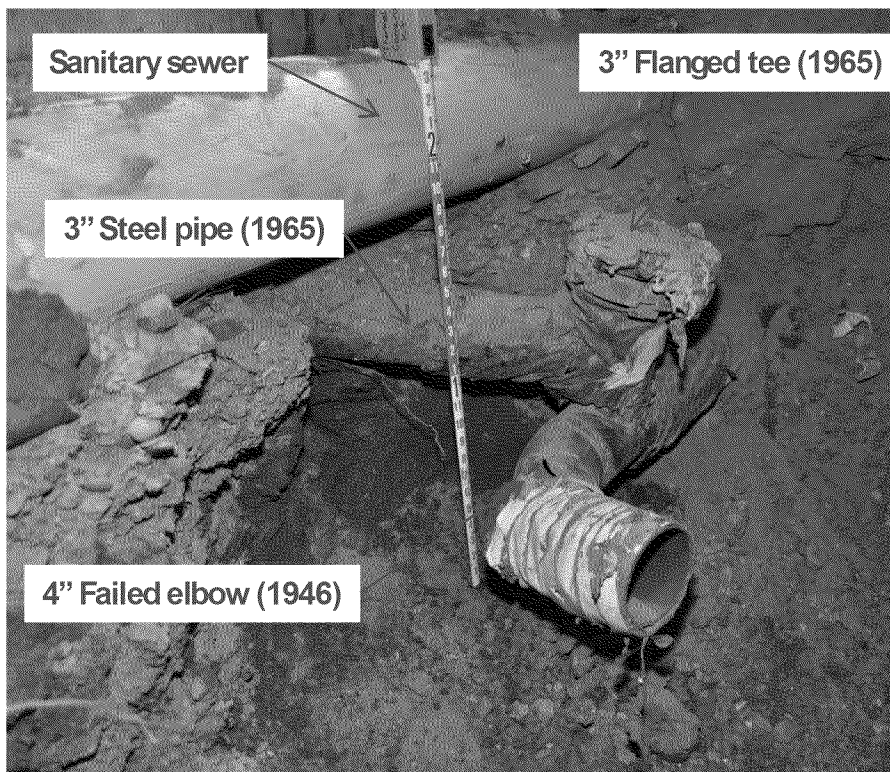


Figure 4. Fractured elbow prior to removal.

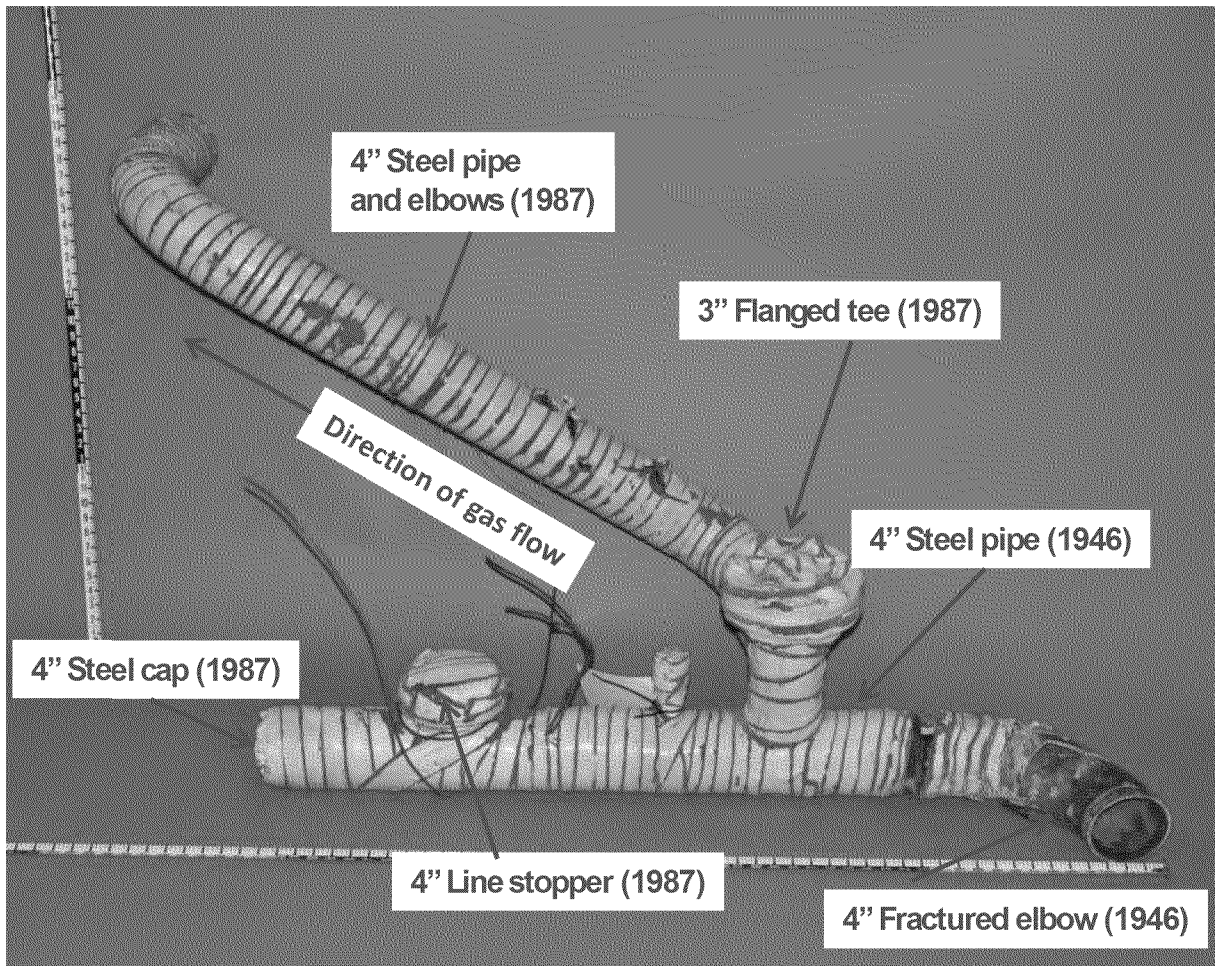


Figure 5. Fractured elbow and adjacent features after removal, with piping photographed as if viewer is looking downstream.

PG&E records show that the gas main has an operating pressure of 48 psig and a maximum allowable operating pressure of 54 psig. The release area was last surveyed for leaks in April 2012 and at that time no leaks were detected in the immediate area of the release.

Gas Distribution Mains, Sewer Line, and Water Line Construction

Exponent reviewed construction drawings provided by PG&E for the distribution gas mains in the area of the gas release. The drawings indicate that the gas pipe in the immediate vicinity of the release was installed during three separate construction jobs:

- G.M.G. 82435 (1946) - Installed a 4-inch diameter steel main along Redacted. This main included two 4-inch steel weld elbows at the location of the leak. One of these weld elbows installed in 1946 failed on December 10, 2013. An as-built construction drawing from G.M.G. 82435 is shown in Figure 6 and Figure 7. The

pipeline features and locations shown in this as-built drawing were consistent with the features in the ground.

- W.O. 4747 (1965) - Installed a 3-inch diameter steel main extending along [Redacted] [Redacted] The 3-inch steel main was connected to the existing 4-inch steel main using a 3-inch flanged tee. A preliminary construction drawing from W.O. 4747 is shown in Figure 8 and Figure 9. This construction drawing has a very low level of detail in the area of the leak. As-built construction drawings for W.O. 4747 were not available to Exponent at the time that this report was issued.
- G.M. 4564829 (1987) - Installed a 4-inch diameter plastic distribution main along [Redacted] [Redacted] starting near the leak site and extending northwest. This main was installed to replace an existing 4-inch steel main. During this job, a piece of 4-inch pipe that was installed in 1946 in the immediate vicinity of the gas release was cut and capped. The 4-inch plastic distribution main was installed with a steel-to-plastic transition, two elbows, and approximately four feet of steel pipe that connected to the existing 1946 4-inch steel main using a 3-inch flanged tee. An as-built construction drawing for G.M. 4564829 is shown in Figure 10 and Figure 11. The pipeline features and locations shown in this drawing were consistent with the features in the ground.

Redacted

Figure 6. As-built construction drawing for job G.M.G. 82435 (1946).

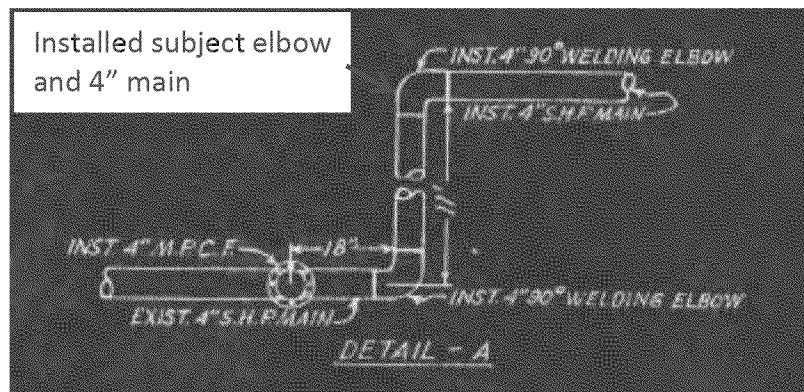


Figure 7. Cropped view of as-built construction drawing for job G.M.G. 82435 (1946) showing area of leak.

Redacted

Figure 8. Preliminary construction drawing for W.O. 4747 (1965).

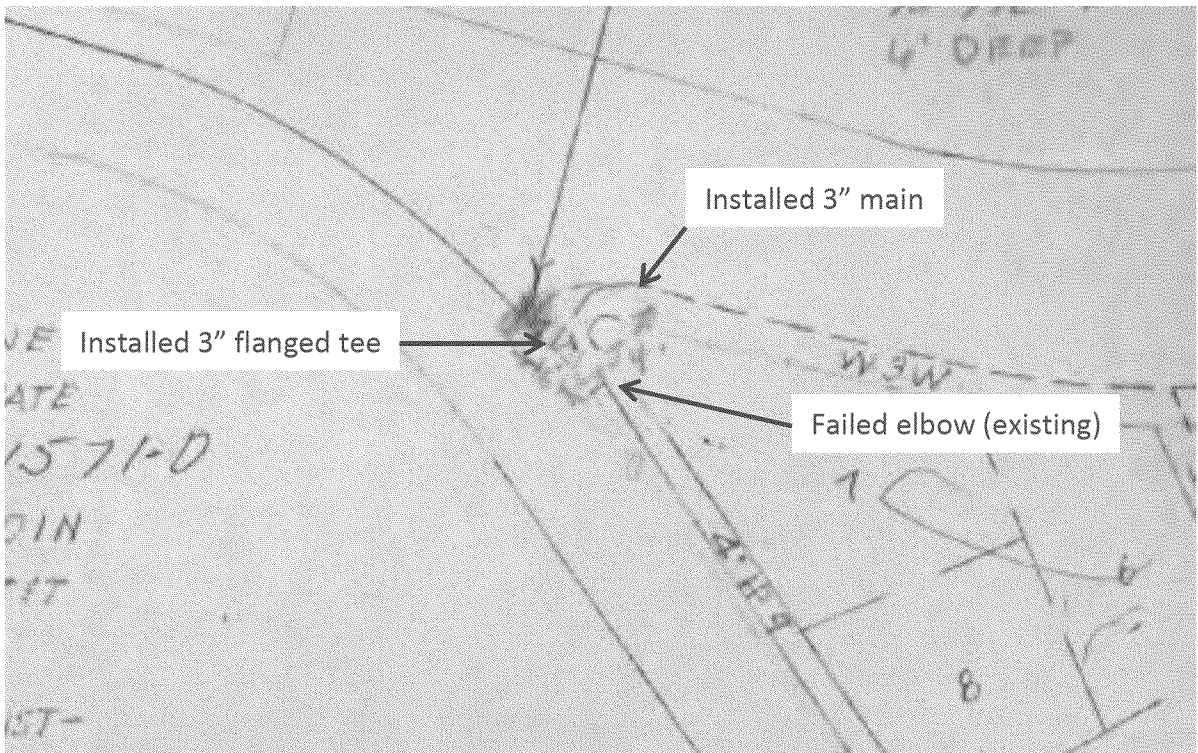


Figure 9. Cropped view of preliminary construction drawing for W.O. 4747 (1965) showing area of leak.

Redacted

Figure 10. As-built construction drawing for G.M. 4564829 (1987).

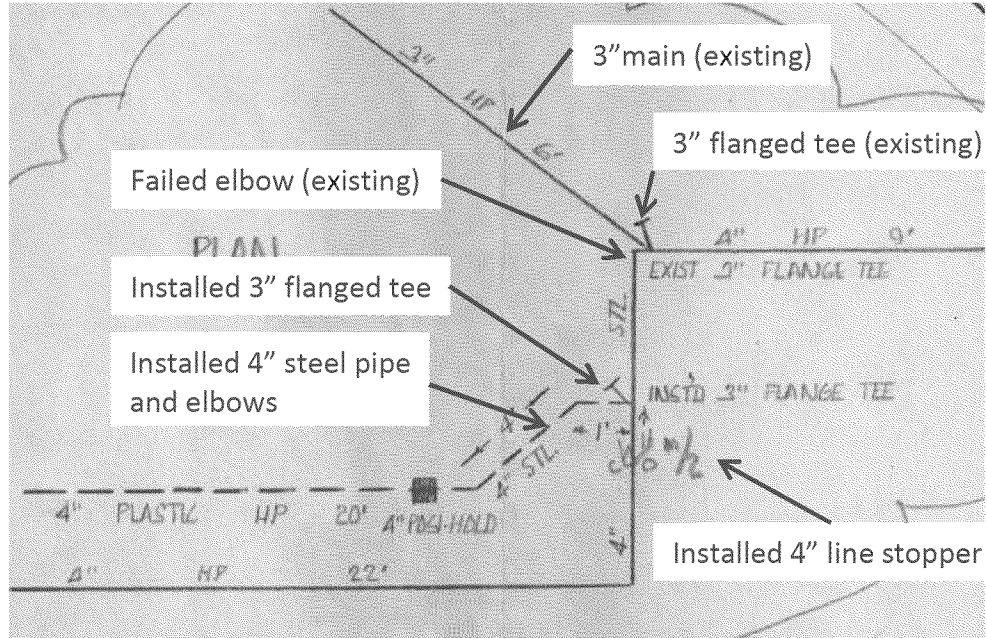


Figure 11. Cropped view of as-built construction drawing for G.M. 4564829 (1987) showing area of leak.

Purchase documentation, shown in Figure 12, was identified for elbows installed on job G.M.G. 82435.

PACIFIC GAS AND ELECTRIC CO.
GENERAL CONSTRUCTION DEPT.
CONSTRUCTION JOURNAL VOUCHER

NOTE: ONE ORIGINAL AND AS MANY COPIES AS ACCOUNTS INDICATED ON DEBIT AND CREDIT SIDES ARE REQUIRED TO BE FORWARDED TO ACCOUNTANT, GENERAL CONSTRUCTION DEPARTMENT.
 CHECK COPY FOR EACH ACCOUNT WITH RED PENCIL.

ITEM NO.	DESCRIPTION GIVE FULL DETAILS OF ALL CHARGES	ITEM NO.	QUANTITY	AMOUNT
	<i>Transferring Material n/a 5/4</i>			
B03E	02 2039, Ell, 4" 90° 1/4 Walling		2	9.74
✓	159026, Electrodes, 1/4" Electrode #5 1lb.		2	15
✓	159024, ✓ 3/16" ✓ 25 lbs		4	36
B03.3	159021, Rod, 3/16" O-cold 1/4 HT Walling		15	1.57
✓	470022, Acetylene C.f.		360	8.34
✓	420027, Oxygen ✓		400	3.86
B03.2	134114, Primer Pacer 3472 Pt2		2	.31
B03.4	ditto ✓		4	.63
1014	Store Expense			2.00
	<i>projected</i>		TOTAL	27.03

I CERTIFY THAT THE MATERIAL LISTED ON THIS DOCUMENT HAS BEEN RECEIVED AND USED ON G.M.G. 82435.
 ITEM NO. [Redacted] [Redacted]
 [Redacted] [Redacted]
 [Redacted] [Redacted]

MONTH OF *November* 194*6*

DEBIT THE FOLLOWING ACCOUNTS IN THE AMOUNT SHOWN	CREDIT THE FOLLOWING ACCOUNTS IN THE AMOUNT SHOWN
<i>6196 82435</i> <i>27.03</i>	<i>145 Micro Materials</i> <i>27.03</i>

[Redacted] [Redacted]

Figure 12. Construction journal voucher for 4-inch weld elbows on G.M.G. 82435 (1946).

The construction journal voucher shown in Figure 12 indicates that two weld elbows with a material code of 02-2039 were installed on G.M.G. 82435. These are likely the elbows shown in Figure 7, one of which is the subject elbow. PG&E gas standards from 1952 show that this material code corresponds to a 4-inch weld elbow with a wall thickness of 0.237 inches. Measurements of the wall thickness of the incident elbow were taken at multiple locations. The minimum measured wall thickness was 0.215 inches and the maximum measured wall thickness was 0.297 inches.

The nearby water main lateral, shown in Figure 3 and Figure 13, was located near the 4-inch steel gas main that was installed in 1987. This water line likely feeds a fire hydrant adjacent to the gas release site. The water lines in the area are owned by the East Bay Municipal Utility District (EBMUD). Per information provided to PG&E by EBMUD, there are three water mains under [Redacted]: an 8-inch main installed in 1961, a 36-inch diameter main installed in 1957, and a 48-inch diameter main installed in 1962. EBMUD has reportedly experienced water main failures in the immediate vicinity about once every ten years. EBMUD believes that landslides and the Hayward Fault are the primary external loading factors that contributed to the failures.



Figure 13. Water main lateral and sanitary sewer.

The nearby sanitary sewer line, shown in Figure 4 and Figure 13, was located near the 3-inch steel gas main that was installed in 1965. The existing sewer line appears to have been installed by slip lining or pipe bursting an older clay sewer pipe. Pieces of broken red clay pipe were observed to surround the plastic sewer main as shown in Figure 4 and Figure 13. Sewer maps from the City of Oakland, last revised on 8-25-2004, indicate that the sanitary sewer at [Redacted] [Redacted] and [Redacted] was rehabilitated and the City of Oakland has records indicating the as-built date as 2003.

Ignition Source Analysis

Exponent conducted site inspections at the area of gas release, including two inspections on December 10 and December 11, 2013, and performed an assessment of possible ignition sources for the incident fire. The possible ignition sources identified include pipeline electrolysis test stations (ETS), [Redacted], utility poles, passing automobiles, and other unidentified transient ignition sources. The locations of possible ignition sources are shown in Figure 14.

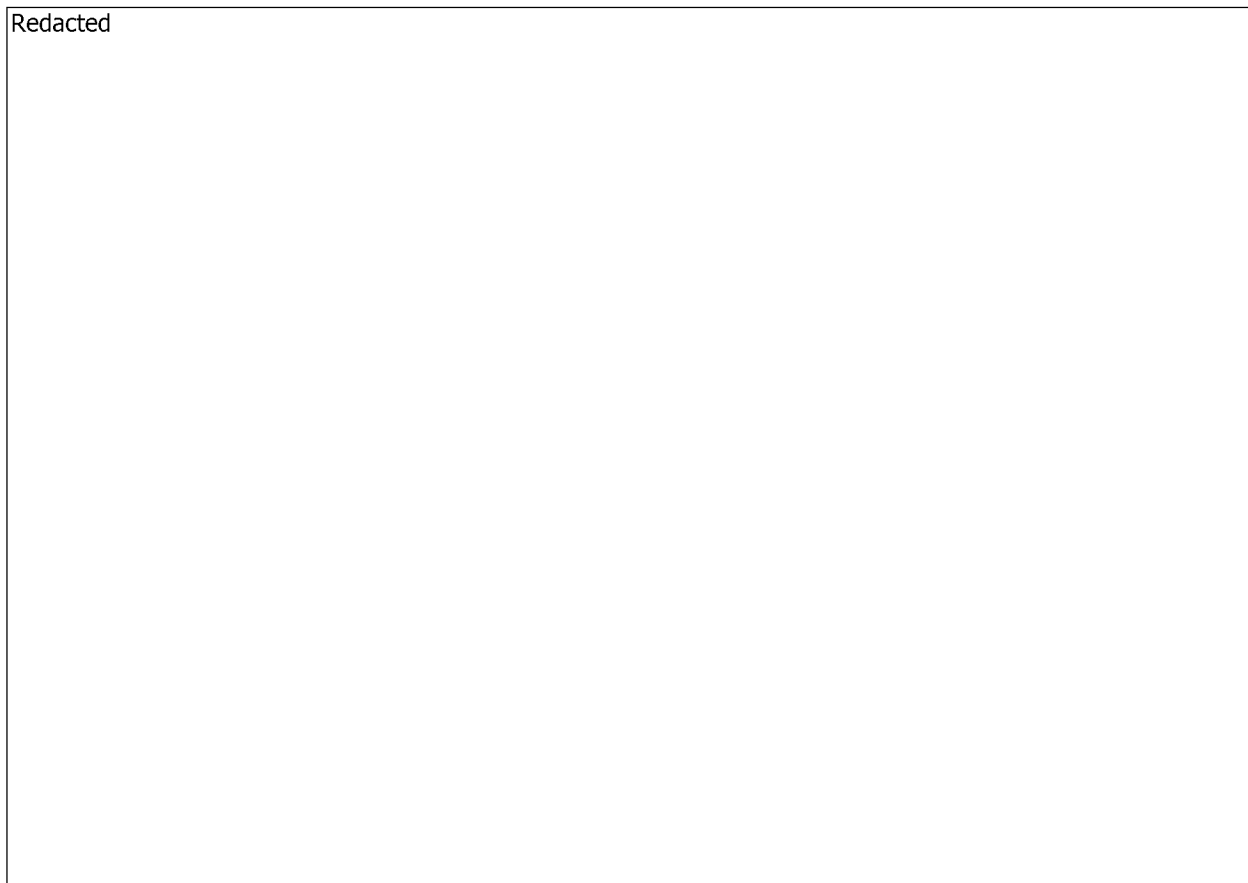


Figure 14. Locations of possible ignition sources.

Each potential ignition source was assessed and the conclusions are described in the following sections.

Passing automobile – Electrical sparks in an automobile engine compartment, mechanical sparks from road debris or a dragging chain, or engine backfires could provide a competent ignition source. The fractured elbow was located directly underneath a paved street and near a busy intersection. Additionally, the fire was first reported at approximately 8:39 a.m., which is during peak hours for the morning traffic commute. For these reasons, a passing automobile cannot be ruled out as a possible ignition source.

EBMUD ETS – An EBMUD vault containing an ETS for assessing the cathodic protection of the water main was identified near the gas release site. Per EBMUD, the water mains in the area of the leak are protected by means of a buried magnesium galvanic anode. This type of cathodic protection system will not create a competent ignition source. Additionally, inspection of the vault showed that the fire damage is consistent with an external fire attack and is not consistent with an internal fire or explosion. Thus, it is unlikely that the EBMUD ETS vault was the ignition source for the incident fire.

PG&E ETS – A PG&E ETS was identified near the gas release site. Gas pipeline cathodic protection systems typically result in potentials on the order of -800mV to -1200 mV. The voltage and currents utilized in the PG&E cathodic protection system are unlikely to create a competent ignition source. Additionally, no damage or displacement of the ETS cover was observed that would be consistent with an internal ignition event or explosion. Thus, it is unlikely that the PG&E ETS was the ignition source for the incident fire.

Electric Vaults – Four PG&E electric vaults were identified near the area of gas release. No physical damage or displacement of the covers that would typically be consistent with an internal ignition or explosion was observed on the exterior of the vaults. An internal inspection by PG&E after the incident showed no signs of an internal failure. It is unlikely that an electrical vault was the ignition source for the incident fire.

Phone Vaults – Two phone vaults were identified near the area of gas release. No physical damage or displacement of the covers that would typically be consistent with an internal ignition or explosion was observed on the exterior of the vaults. It is unlikely that one of the phone vaults was the ignition source for the incident fire. Examinations of the interiors of the phone vaults for burn damage or component failure could confirm this conclusion.

Cable Vaults – Two cable vaults were identified near the area of gas release. No physical damage or displacement of the covers that would typically be consistent with an internal ignition or explosion was observed on the exterior of the vaults. Additionally, the area immediately surrounding the cable vaults did not show any signs of fire damage. It is unlikely that one of the cable vaults was the ignition source for the incident fire. Examinations of the interiors of the cable vaults for burn damage or component failure could confirm this conclusion.

Utility Pole – A utility pole was identified near the area of the gas release. The distance between the failed elbow and possible ignition sources on the utility pole would require a significant gas cloud to form in order for ignition to occur. Ignition of such a gas cloud would typically cause a large fireball, loud audible sounds, and potentially damaging overpressures to nearby structures. There is no indication that this occurred. It is unlikely that the utility pole or any of the components mounted near the top of the pole was the ignition source for the incident fire.

Other/Unidentified – Numerous transient ignition sources could have been present at the time of the gas release. These include a discarded cigarette, electrostatic discharge, or other unidentified ignition sources. The area of the gas release is a publicly accessible space with

frequent vehicle traffic. Thus, an unidentified transient ignition source cannot be ruled out as the ignition source for the incident fire.

Based on this analysis, a passing automobile or other/unidentified transient ignition source are possible ignition sources. These possible ignition sources and the conclusions reached are summarized in Table 1.

Table 1. Potential ignition sources.

Potential Ignition Source	Conclusion
Passing automobile	Possible
EBMUD ETS	Unlikely
PG&E ETS	Unlikely
Electric vault	Unlikely
Phone vault	Unlikely
Cable vault	Unlikely
Utility pole	Unlikely
Other/Unidentified	Possible

Metallurgical Failure Analysis

Visual Examination

The ruptured elbow and piping downstream from the break was removed from the leak site as shown in Figure 5, and was brought to Exponent's Menlo Park, California laboratories for analysis. The break occurred at the elbow intrados, as shown in Figure 15. The fracture plane was primarily perpendicular to the gas flow direction and located near the center of the elbow. This fracture orientation is consistent with bending of the elbow, rather than a pressure-induced break. Comparison of the ruptured elbow before and after excavation (Figure 4 and Figure 15) showed that the fracture opened during the excavation process. This is consistent with reports of witnesses on site during the excavation process.

The pipe coating was manually removed from the subject to allow better visual inspection and measurements of the pipe thickness. Areas of pitting corrosion were observed near the top of the elbow, as shown in Figure 16. However, these pitted areas occurred well away from the fracture. No evidence of mechanical damage was observed. No other defects, cracks, seams, weld issues, or anomalies were observed.

The subject elbow was sectioned to allow fractographic and metallographic examination, as well as elbow wall thickness measurements. The minimum wall thickness was 0.215-inch at the 6 o'clock position, and the maximum thickness was 0.297-inch, located at the 10 o'clock position, as shown in Figure 17. All clock positions reported are looking downstream. PG&E construction documents from 1946 and fitting specifications indicated that the subject elbow was specified to have a wall thickness of 0.237-inch, and to be fabricated from ASTM A 106 Grade A or B material. Note that the elbow fractured at the location of greatest wall thickness.



Figure 15. Image of fractured elbow.

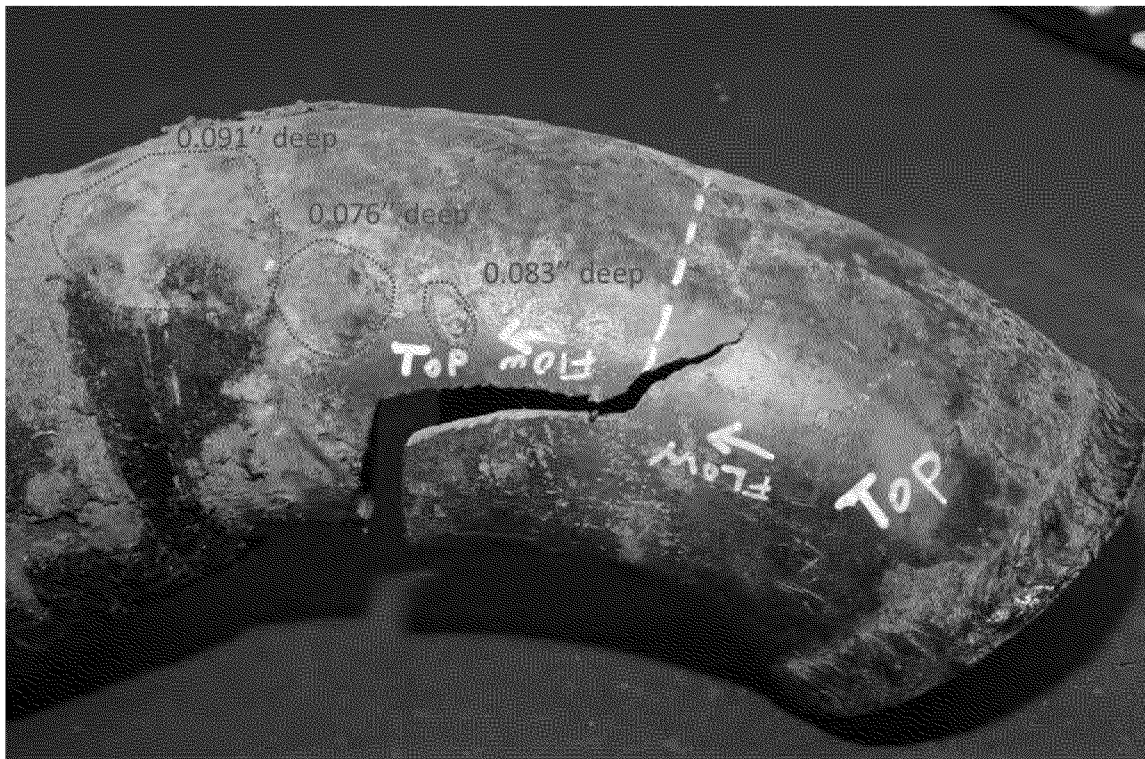


Figure 16. Photograph of the fractured elbow with pipe coating removed showing several corrosion pits, with their depths indicated.

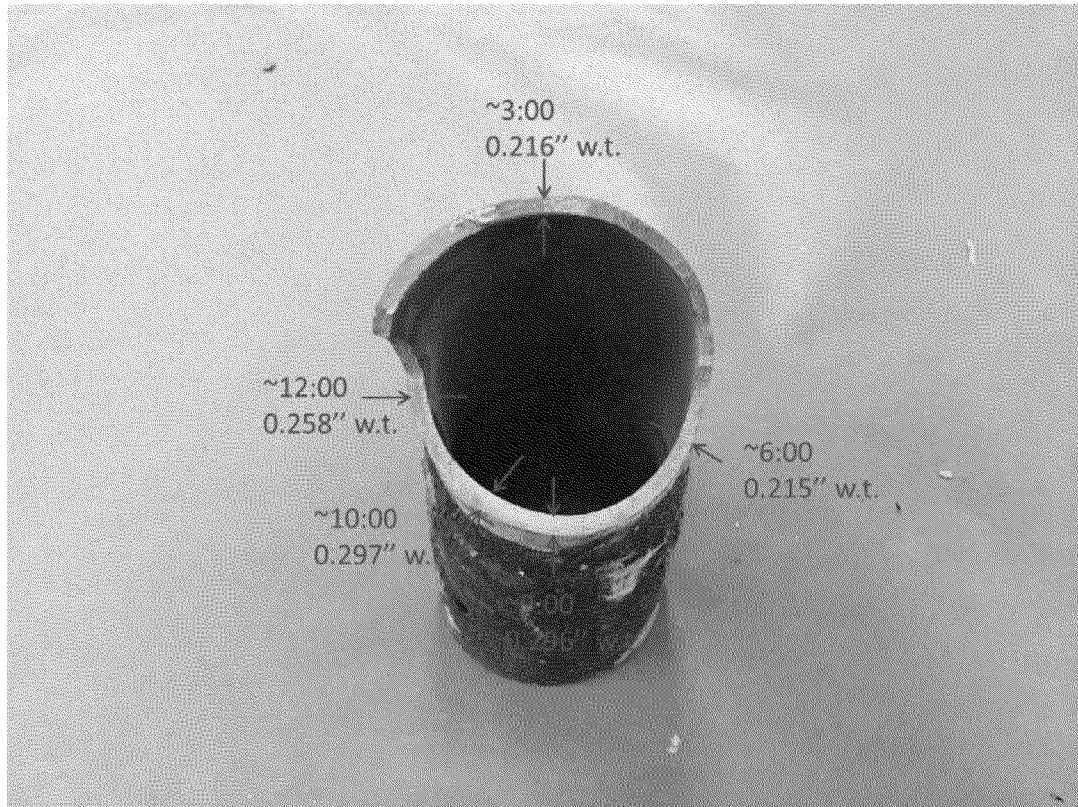


Figure 17. Cross-sectional measurements of pipe thickness around the circumference of the subject elbow at the fracture location.

Fractography

Fractographic analysis was conducted to help determine the cause of the rupture. The elbow was sectioned across the remaining intact area near the break to better expose the fracture surfaces for examination, as shown in Figure 18. To help remove the soil that obscured the surface, the fracture faces were cleaned in a warm Alconox (detergent and water) solution and scrubbed with a nylon brush. Following cleaning, the fracture surface was examined visually as well as using optical and scanning electron microscopy (SEM) techniques. A photograph of the cleaned fracture surface is shown in Figure 19. No dark areas, associated with long-term corrosion, or evidence of progressive fracture (such as beach marks) were observed. The fracture origin area was relatively flat with little ductility. Examination of tear ridges and chevron marks (which point back to the initiation point), shown in Figure 19 and Figure 20, indicated that the fracture origin was located at roughly the 10 o'clock position.

One half of the rupture origin was sectioned from the elbow and examined using SEM to allow identification of the failure mode. The entire fracture area examined, including the origin, exhibited brittle fracture morphology, primarily cleavage fracture, as shown in Figure 21 and Figure 22. Significant smoothing and erosion of the fracture surface was observed using SEM, shown in Figure 21. Fracture surface erosion damage is relatively common in buried pipe

subject to leaking over time, and the amount of fracture surface erosion damage was consistent with the reported duration of the subject leak. The cleavage fracture observed is consistent with brittle fracture morphology in steel subjected to an overstress event.

Consistent with our visual and optical microscope fractographic analysis, no evidence of progressive fracture, such as fatigue or stress corrosion cracking (SCC) was observed. Energy dispersive spectroscopy (EDS) showed no evidence of anomalous elemental species (not shown).

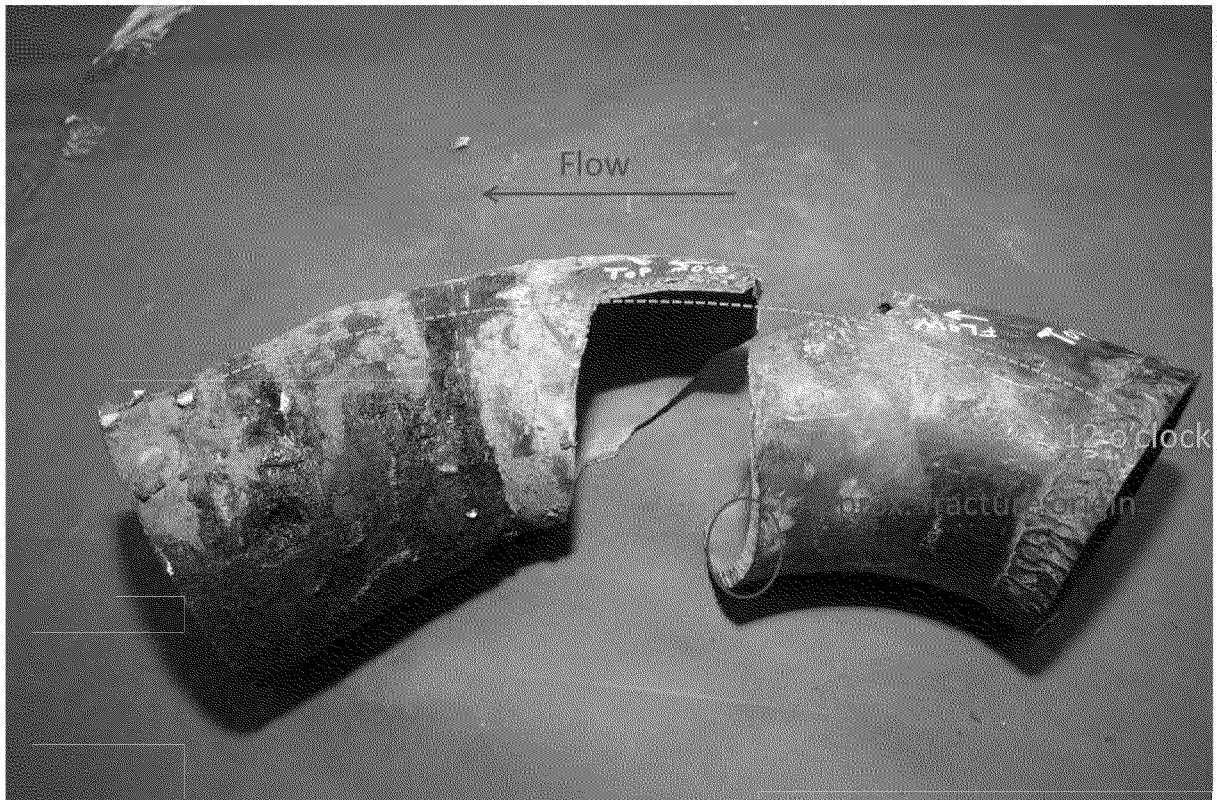


Figure 18. Image that shows the elbow after sectioning. The piece on the right (upstream) was subjected to fractographic and metallographic examination.

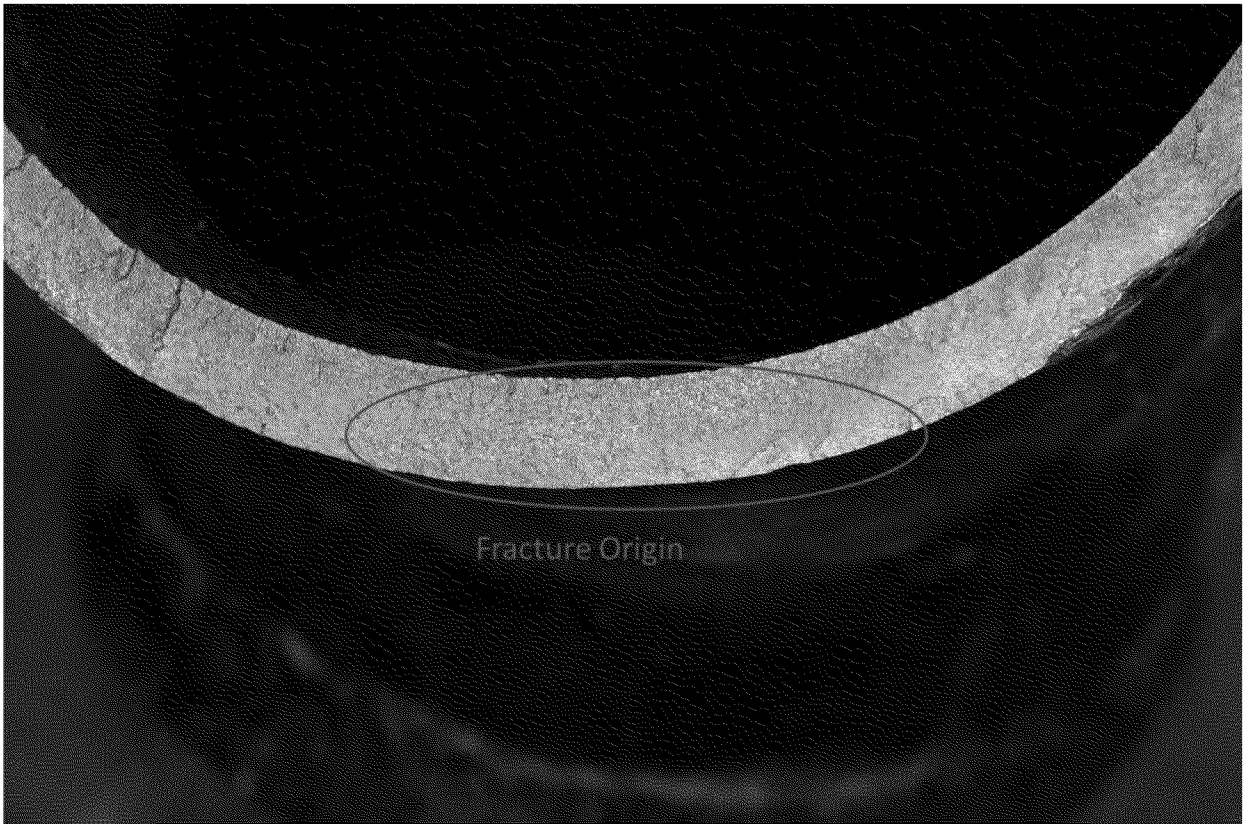


Figure 19. Image that shows the cleaned fracture surface with the fracture origin indicated.

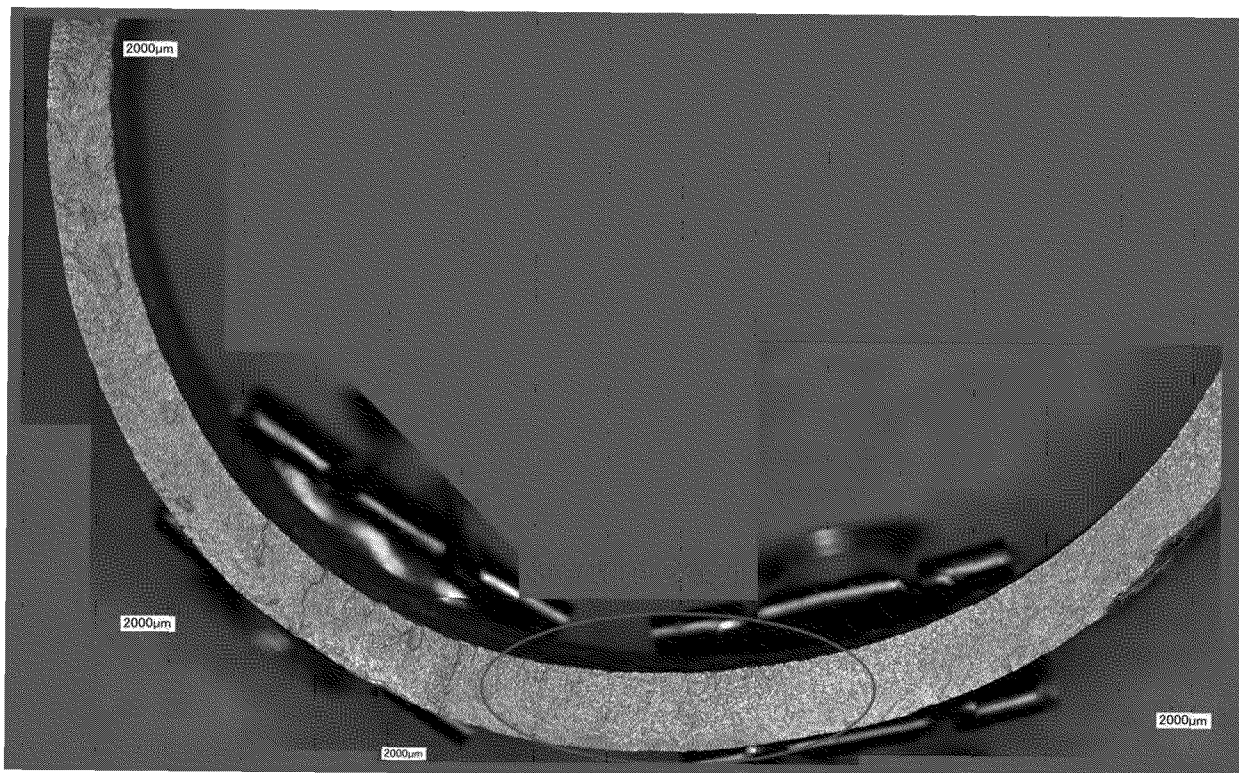


Figure 20. Optical microscope photo montage that shows the fracture surface with the origin indicated.

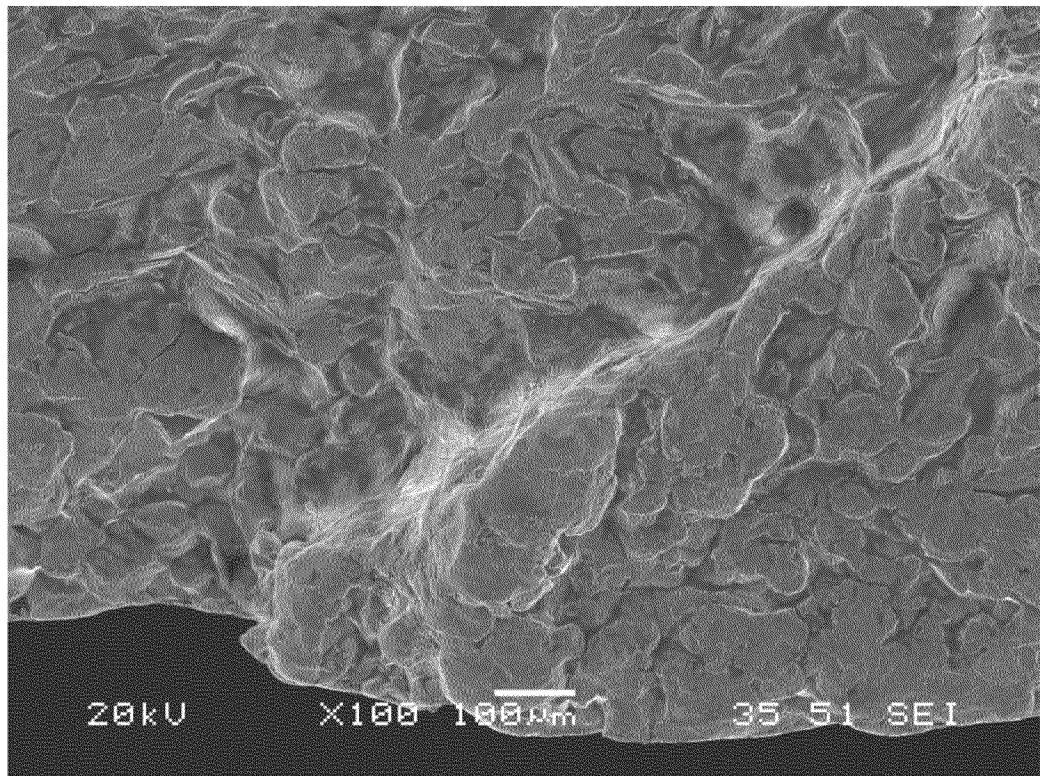
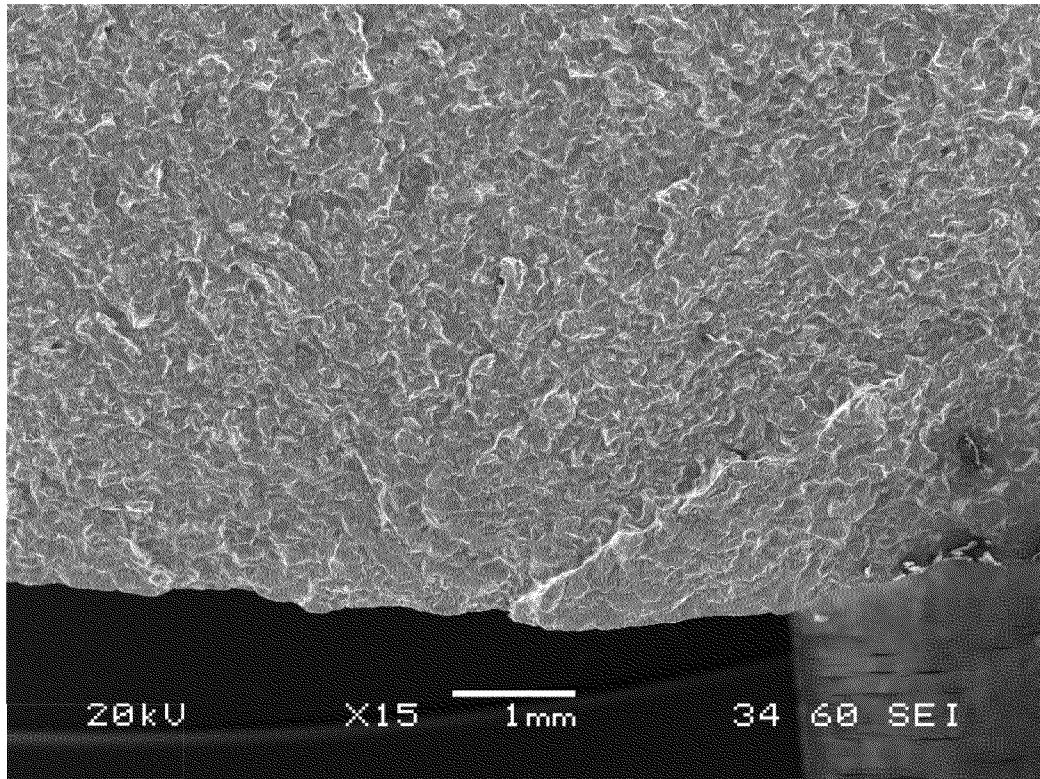


Figure 21. SEM images of the fracture origin showing brittle fracture and erosion from gas release.

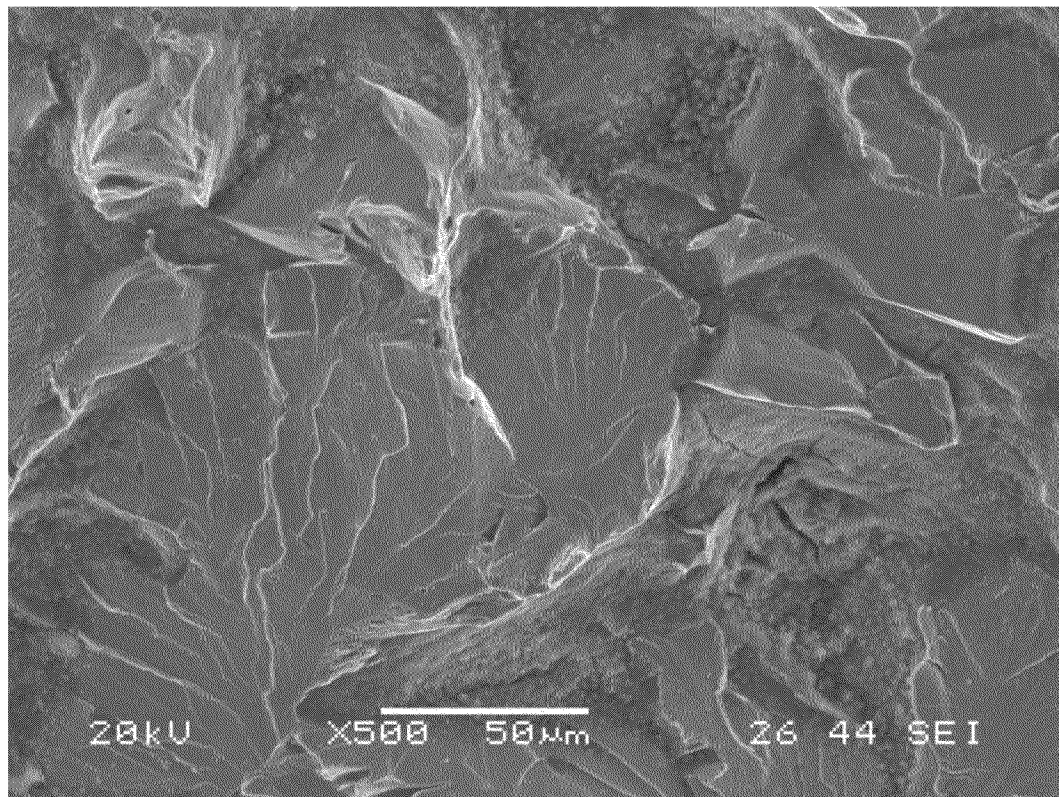
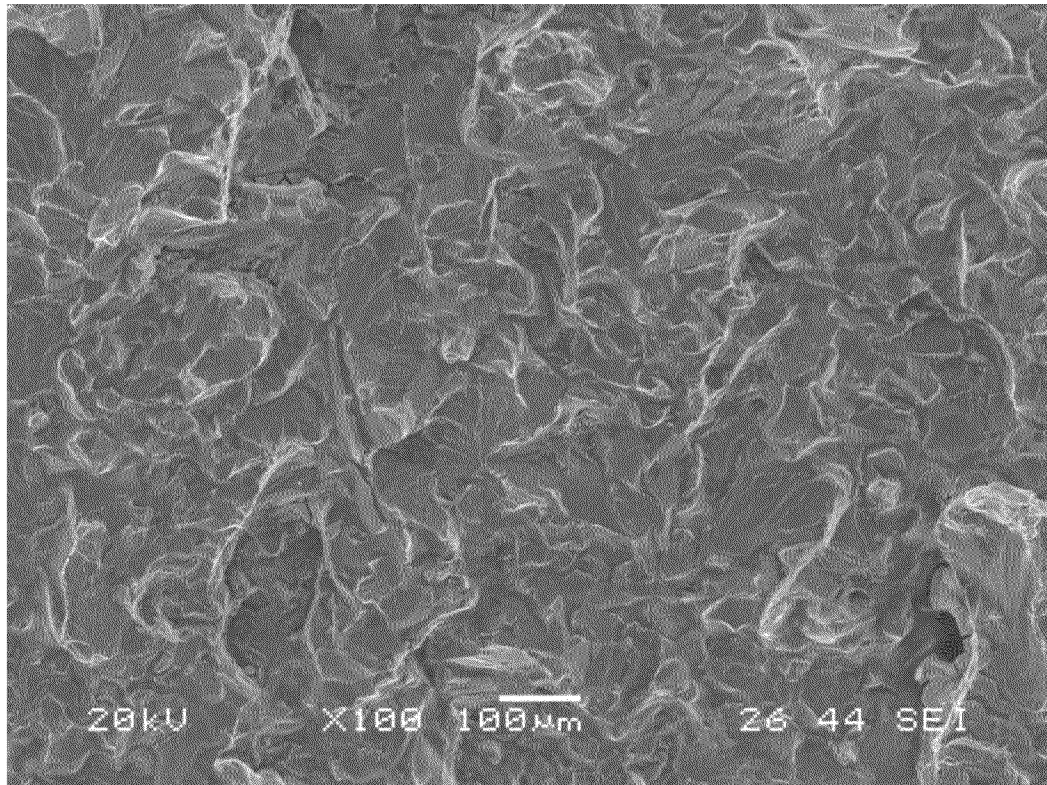


Figure 22. SEM images of varying magnifications of the mid-wall location in the fracture origin region. The fracture morphology shows cleavage, indicative of brittle fracture.

Metallographic Examination

A portion of the fracture origin was sectioned to allow metallographic examination, shown in Figure 23. The sample was mounted perpendicular to the fracture plane (i.e., along the longitudinal direction along the elbow), and was ground, polished, and etched using typical metallographic procedures. The elbow exhibited a typical ferrite and pearlite microstructure, including at the fracture origin, as shown in Figure 24. Microhardness testing was conducted on the metallographic sample: the average hardness was measured to be 193 HV.

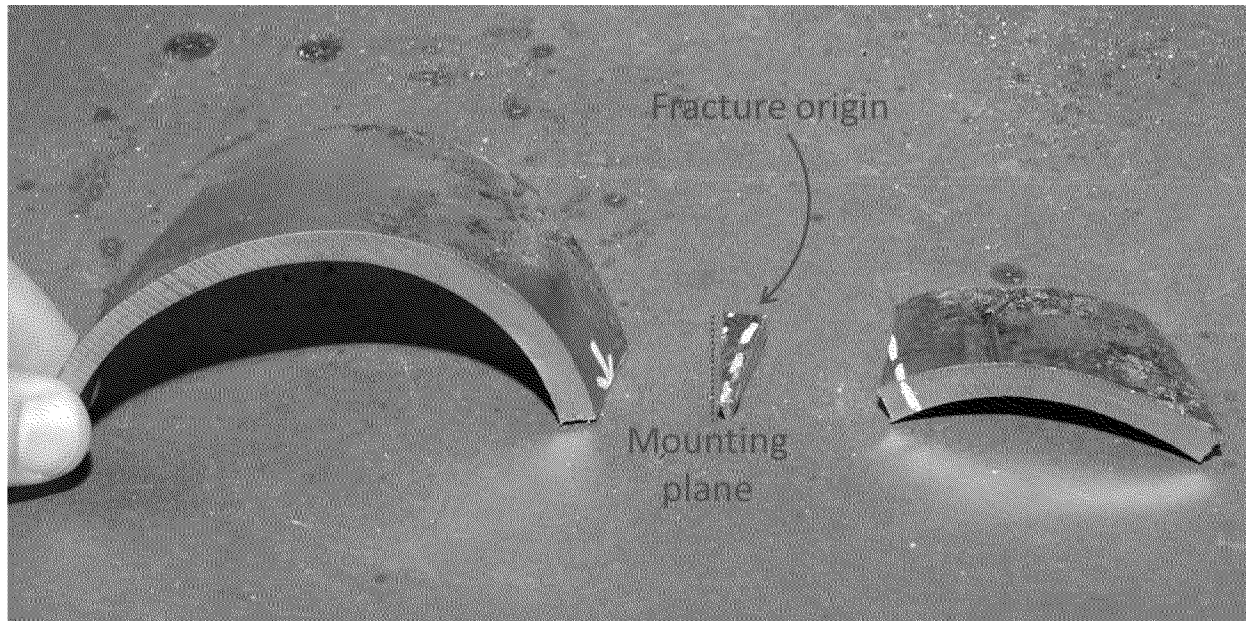


Figure 23. A photograph that shows the metallographic specimen from the origin area.

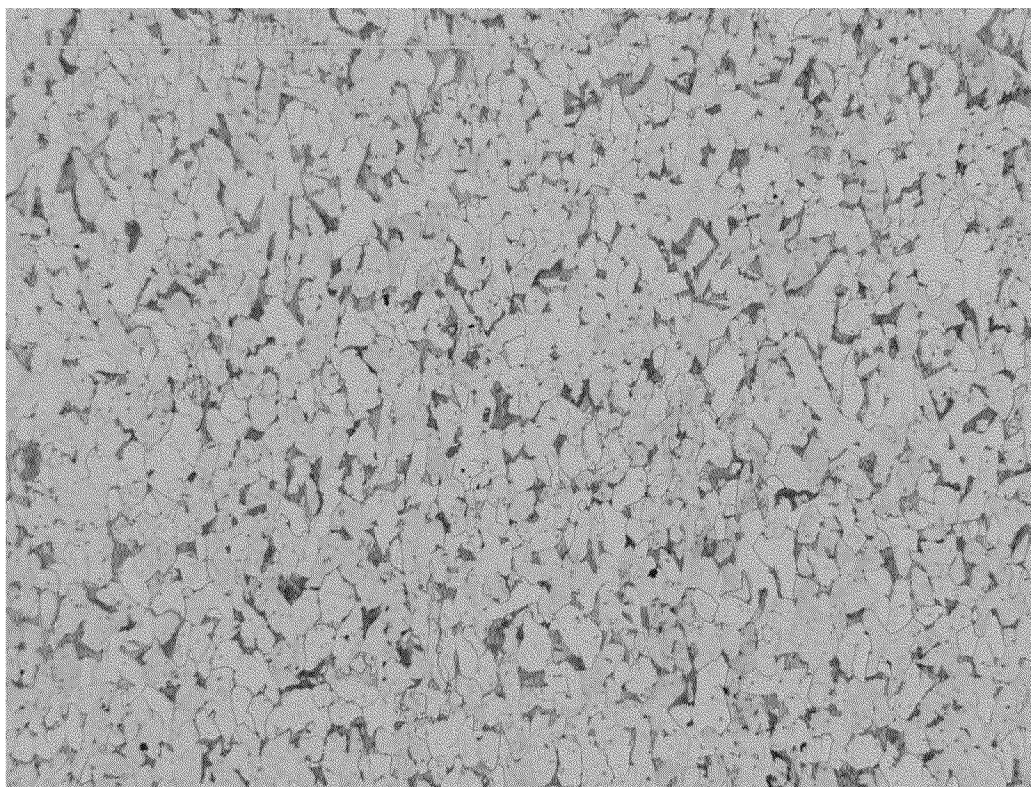


Figure 24. Metallographic image of the elbow ferrite-pearlite microstructure.

Mechanical Testing

Mechanical testing was conducted at Anamet Inc. to compare the subject elbow tensile properties with PG&E specifications.

PG&E drawings 081465 and 281992 specify that 45- and 90-degree elbows should be manufactured in conformance with ASTM A 234,¹ and that material properties should conform to ASTM A 106² Grade A material (Grade B if greater working pressure is needed). These PG&E drawings are dated 1945 and 1952, respectively. ASTM A 106 specified Grade A tensile and yield strengths to be 48 and 30 ksi, respectively; while Grade B tensile and yield strengths were specified to be 60 and 35 ksi, respectively. Due to the small size of the tensile specimens removed from the subject elbow, a minimum transverse elongation is not required.

Anamet's reports are provided in Appendix A. Tensile test specimens were removed from two locations: two from the downstream, extrados area of the subject elbow; and two from the straight pipe section directly downstream from the broken elbow. As shown in Table 2, tensile test results indicate that the elbow met the strength requirements for ASTM A 106 Grade A and

¹ ASTM A 234, Factory-Made Wrought Carbon Steel and Ferritic Alloy Steel Welding Fittings (1952).

² ASTM A 106, Tentative Specifications for Lap-Welded and Seamless Steel Pipe for High-Temperature Service (1942).

B specifications. Tensile samples cut from the elbow were too thin to conform with the minimum quarter-inch thickness requirement for ASTM A 106 Grade A and B transverse tensile specimen elongation. The straight segment of pipe met specifications for API 5L Grades A and B.

Table 2. ASTM A370-10 tensile test results.

Specimen ID	Elbow or Pipe Specimen	Tensile Strength (ksi)	Yield Strength 0.2% Offset (ksi)	Yield Strength 0.5% E.U.L.(ksi)	Elongation in 1-inches (%)	Elongation in 2-inches (%)
109035 – 1	Elbow	75.6	62.6	n/a	19	n/a
109035 – 2	Elbow	77.0	57.7	n/a	19	n/a
109241 – 1	Pipe	65.2	51.5	51.6	n/a	20.5
109241 – 2	Pipe	64.6	51.7	51.3	n/a	22.5
ASTM A106 Grade A/ B		48/ 60	30/ 35			
API 5L 1949 Grade A/ B		48/ 60	30/ 35			20

Chemical Analysis

Specimens for chemical analysis were removed from both subject elbow and adjacent pipe sections for comparison with appropriate ASTM and API specifications. The results indicate that the subject elbow and adjacent pipe met the pertinent chemistry requirements.

Table 3. Quantitative chemical analysis test results.

Element	109035 (elbow) (weight %)	109241 (pipe) (weight %)	ASTM A106 Grade A	API 5L 1949 Grade C Spec. (wt. %)
Aluminum	0.01	<0.005		
Carbon	0.13	0.27	0.25 max	0.30 max
Chromium	0.01	0.04		
Copper	0.02	0.07		
Iron	Main Constituent	Main Constituent		
Manganese	0.42	0.63	0.30 - 0.90	0.35 - 1.50
Molybdenum	<0.005	0.01		
Nickel	0.02	0.08		
Phosphorus	0.007	0.011	0.04 max	0.045 max
Silicon	0.16	<0.005		
Sulfur	0.018	0.054	0.06 max	0.060 max
Titanium	<0.005	<0.005		
Vanadium	<0.005	<0.005		

Metallurgical Discussion

Metallurgical analysis indicates that the Redacted release occurred when external forces acting on the piping resulted in stresses that exceeded the subject elbow's tensile strength. Visual inspection indicated that no corrosion, mechanical damage, or manufacturing defects contributed to the break. Optical microscope and SEM analyses indicated that no progressive crack growth, such as fatigue or SCC, had occurred. Metallographic analysis indicated no microstructural discontinuities associated with the subject elbow. Mechanical and elemental testing indicated the subject elbow met appropriate standards for tensile and chemical properties.

Geotechnical Analysis

Physical Setting

Exponent’s geotechnical scope of work is summarized in Appendix B. The gas release site (“Site”) is located at the intersection of [Redacted] and [Redacted], just upslope from the base of the Oakland hills and west of [Redacted] as shown in Figure 25. The general topographic, drainage and geologic setting of the Site are summarized in Appendix C.



Figure 25. Location map. Source: USGS, 2012, Oakland East Quadrangle, California, 7.5-minute series, scale 1:24, 000.

Summary of Ground Movement Mechanisms Evaluated

Exponent evaluated possible ground movement mechanisms in the vicinity of the Site. Those mechanisms included fault-creep ground deformation, recent seismic activity, non-seismic ground settlement, and landslide movement. Each of those mechanisms is discussed in the following sections.

Fault-Creep Ground Deformation

The Site is located within the active Hayward Fault Zone. Exponent assessed the likelihood of fault creep causing external forces on the pipe system at the Site, as discussed in the following subsections.

Hayward Fault Characteristics

The Hayward Fault is part of the boundary between the North American and Pacific tectonic plates. The fault is a right-lateral strike-slip fault,³ as shown in Figure 26. Most major active faults, including the Hayward Fault, are characterized by zones of multiple subparallel fault traces with varying degrees of activity.

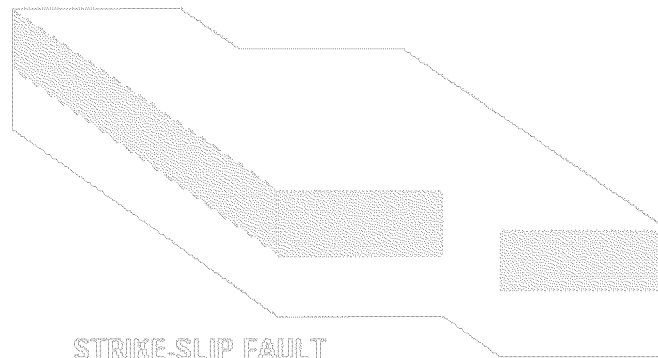


Figure 26. Block diagram showing right-lateral strike-slip fault. Source: Pridmore, Cindy, 1992, California has its faults... *in* California Division of Mines and Geology, California Geology magazine, January/February 1992, http://www.consrv.ca.gov/cgs/information/publications/teacher_features/pages/faults.aspx

The last major earthquake on the Hayward Fault occurred in 1868. According to the USGS, the 1868 magnitude 6.8 earthquake was accompanied by a surface rupture that “was traced for 20 miles along the Hayward Fault, from Warm Springs in Fremont north to San Leandro. Historical land-survey data suggest that the fault broke as far north as Berkeley, with an average horizontal movement of about 6 feet (2 meters).”⁴ This rupture extent includes the vicinity of the Site.

³ “Right-lateral strike-slip” means that displacement along the fault is predominantly horizontal (“strike-slip”) and when looking across the fault, the sense of movement of the opposite side is to the right (“right-lateral”).

⁴ Brocher, T.M., Boatwright, Jack, Lienkaemper, J.J., Prentice, C.S., Schwartz, D.P., and Bundock, Howard, 2008, The Hayward Fault - is it due for a repeat of the powerful 1868 Earthquake?: USGS, Fact Sheet 2008-3019, 4 p. <http://pubs.usgs.gov/fs/2008/3019/>

The Hayward Fault was designated as an active fault by the State of California Alquist-Priolo Earthquake Fault Zoning Act of 1972.⁵

One piece of evidence of the location of the Hayward Fault at the Site is a right-lateral offset of a tributary stream channel (see Appendix C) emphasized by the storm-drain alignments following the old stream channel in Figure 27. The stream offset likely represents the location of one trace of the Hayward Fault, but not necessarily the active trace, which will be discussed in the next section.

In addition to episodic earthquakes - seismic events - the Hayward Fault experiences fault creep. Fault creep is gradual, aseismic fault movement that typically occurs between episodes of sudden seismic fault movement which causes earthquakes. Most faults remain locked and do not creep between earthquakes. The Hayward Fault, however, is an actively creeping fault.

⁵ Bryant, W.A. and Hart, E.W., interim revision 2007, Fault-Rupture Hazard Zones in California, California Geological Survey Special Publication 42, 42 pgs, <ftp://ftp.consrv.ca.gov/pub/dmg/pubs/sp/Sp42.pdf>.

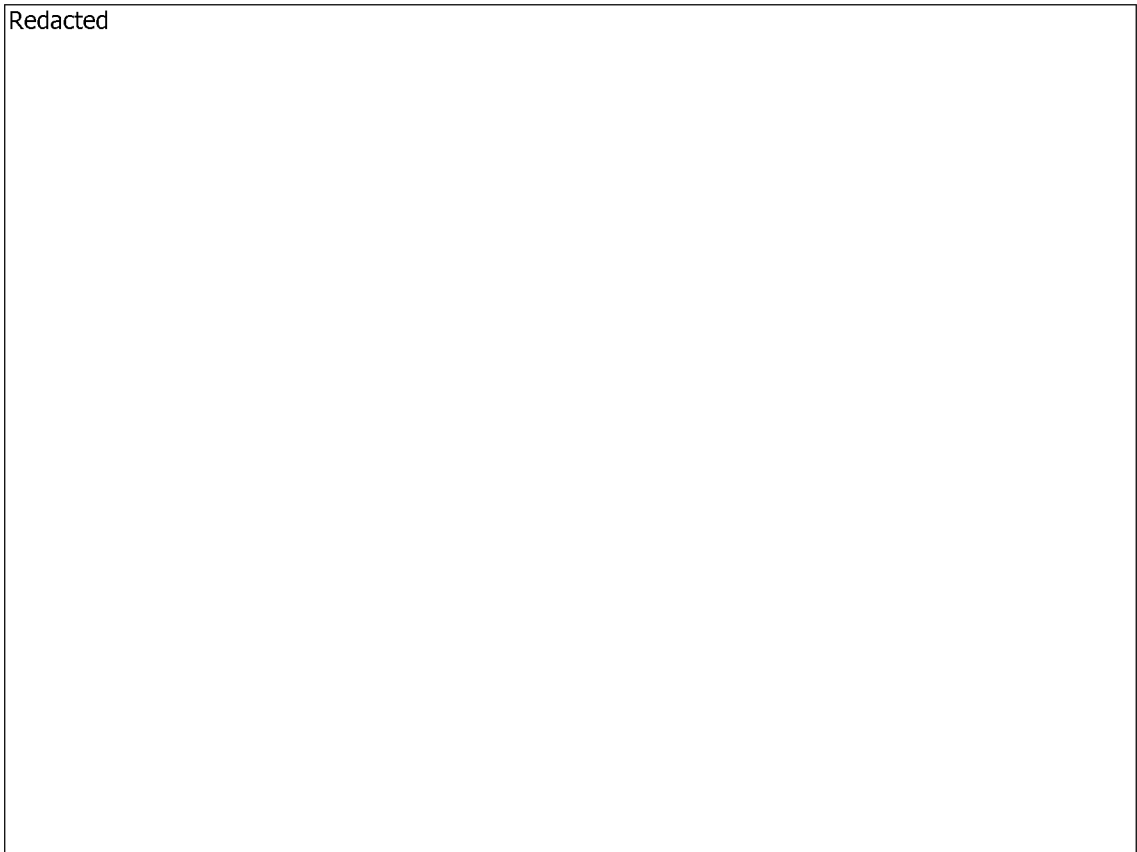


Figure 27. City sewer map overlaid on pre-Redacted topography (see Appendix C). Black arrow indicates culvert under Redacted. Yellow highlighting indicates storm-drain segments along offset stream channel. Sources: City of Oakland Underground Sewer Maps, Sheets 92 and 93, last revised 8-25-2004, scale unknown; City of Oakland topographic map excerpt; title, date, and scale unknown; from Building Services Division Land Stability File 92 L/4, "Grading, 8467 & 8475 Redacted Redacted 1 of 2."

Location of Active Fault Trace

To investigate fault movement, including fault-creep rates, numerous studies have been performed on the Hayward Fault. One such study mapped "the location of and evidence for recent movement on active fault traces within the Hayward Fault Zone, California."⁶ A portion of this map, overlaid on an aerial image of the vicinity of the Site, is shown in Figure 28. The map shows numerous locations where evidence of fault creep has been observed in the vicinity of the Site.

⁶ Lienkaemper, J.J., 2006, revised 2008, Digital database of recently active traces of the Hayward Fault, California: USGS DS-177, <http://pubs.usgs.gov/ds/2006/177/>

Lienkaemper (2006, revised 2008) stated that the accuracy of the mapped location of active fault traces varies throughout the mapped fault zone. In the vicinity of the Site, the actual active trace of the Hayward Fault is interpreted to be within 60 meters of the line shown on the map. Figure 29 shows the approximate area in which the active trace of the Hayward Fault is interpreted to be located, according to the Lienkaemper map. As shown on this figure, the Site is well within the mapped location of the active Hayward Fault trace. Figure 29 also shows the approximate direction of right-lateral displacement of the Hayward Fault in the vicinity of the Site. Figure 30 shows a plan view of the approximate configuration of the pipe system exposed during repairs and the pipe rupture location. The figure also shows the approximate direction of right-lateral movement of the Hayward Fault in the vicinity of the Site.

As discussed later in this report, the presence of a large ancient landslide near the Site obscures some surface traces of the Hayward Fault. The presence of this landslide likely contributed to the relatively large uncertainty in the location of the Hayward Fault near the Site (i.e., actual active trace of the fault within 60 meters of the line shown on the map).

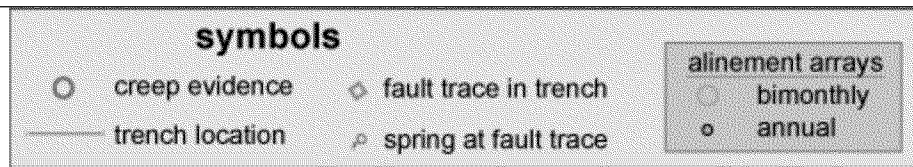
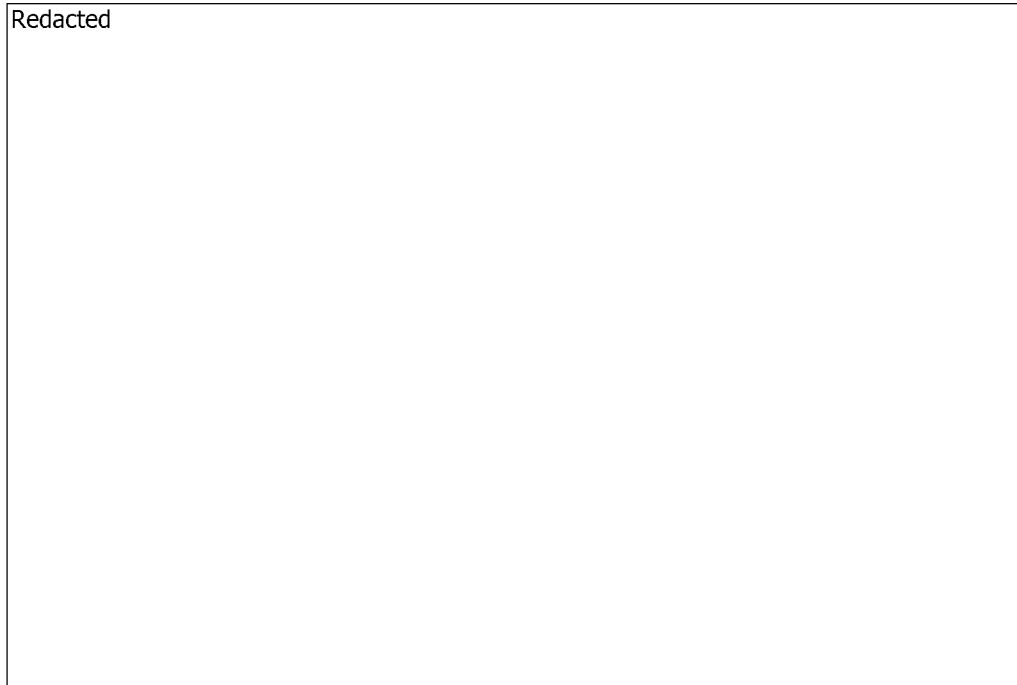


Figure 28. Map showing recently active trace of Hayward Fault in vicinity of Site. Sources: Lienkaemper, J.J., 2006, revised 2008, Digital database of recently active traces of the Hayward Fault, California: USGS DS-177, <http://pubs.usgs.gov/ds/2006/177/> overlain on 2012 Google Earth air photo.



Figure 29. Aerial photograph showing approximate location of recently active trace of Hayward Fault in immediate vicinity of Site. Red box indicates width of zone of uncertainty within which the active fault trace is interpreted to be located. Sources: Google Earth; Lienkaemper (2006, revised 2008) <http://pubs.usgs.gov/ds/2006/177/>.

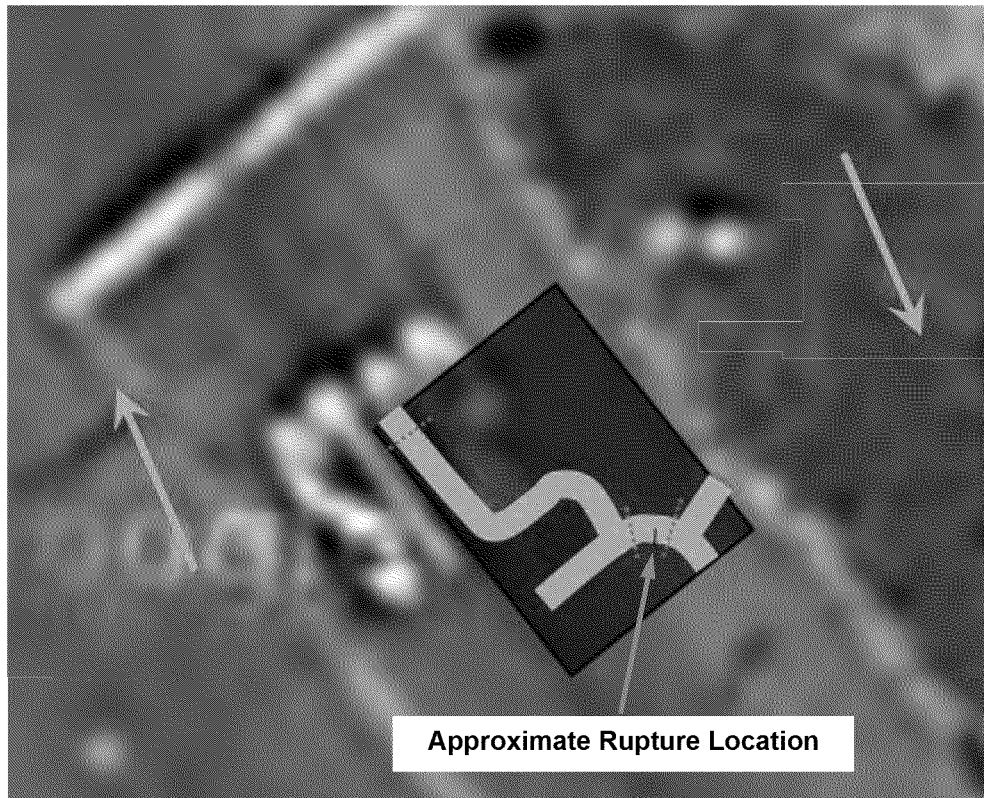


Figure 30. Plan view of pipe system exposed during repairs. Arrows indicate approximate direction of right-lateral movement of Hayward Fault in the vicinity of the Site. Photograph source: Google maps.

Width of Fault-Creep Zone

The zone containing the likely location of the actively creeping fault trace (Figure 28 and Figure 29) is not to be confused with the fault-creep deformation zone. The deformation zone can be wider or narrower than the zone of uncertainty on the actual creeping trace location. Evaluations of the width of the fault-creep zone at the Site are described in the following section.

Exponent Observations

Exponent's project geologist and/or project civil engineer performed visits to the Site on December 13 and 17, 2013, and January 3, 2014 to look for surface evidence of ground movement, including fault creep. No definitive field evidence of creep was present at the Site or on nearby streets that cross the Hayward Fault. The southern portion of the retaining wall on the north side of [Redacted] (Figure 29), however, exhibited a prominent crack (Figure 31) and a separation at a joint (Figure 32), both of which had a right-lateral sense of displacement. In the case of the crack, the displacement was greater at the base of the wall (approximately ½-inch) than at the top. This configuration of retaining wall cracking may well represent displacement of the base of the wall by fault creep.

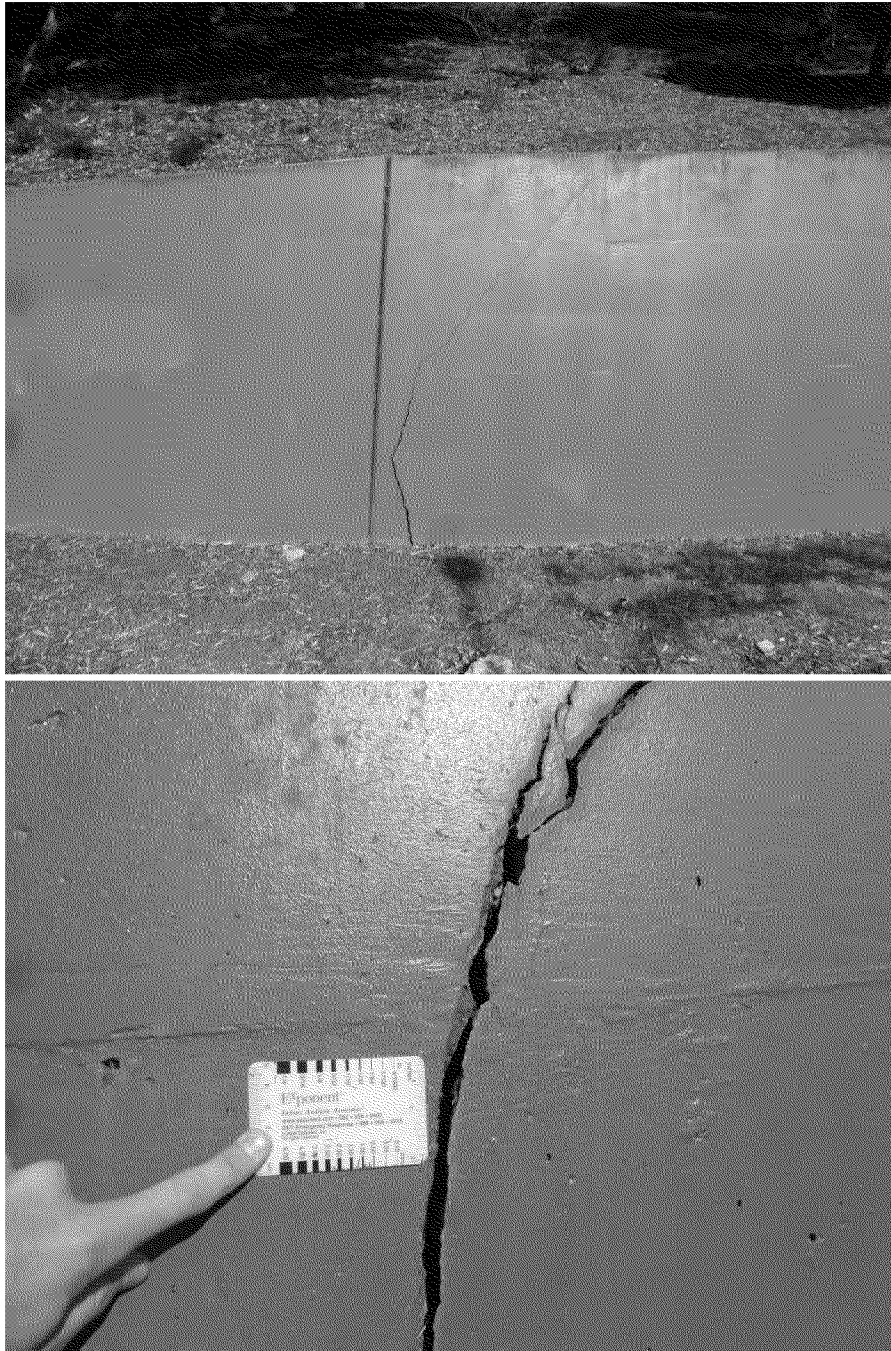


Figure 31. Retaining wall crack, looking north. Photographs by Exponent, December 13, 2013.



Figure 32. Displaced retaining wall joint. Oval encloses observed recent soil deposits near the base of the wall. Arrow indicates right-lateral displacement at top of wall. Photographs by Exponent, December 13, 2013.

More definitive evidence of creep was observed on both sides of Redacted, approximately 900 meters southeast of the Site. This area is the location of an alignment array next to the

Redacted

as shown in Figure 28. The displacements shown in the photograph in Figure 33 are two of three right-lateral displacements of the sidewalk, curb, and gutter observed along the northwestern side of the street. The distance between the first and last (third) displaced joints was approximately 15 feet. The curb on the opposite side of the street was also displaced right laterally.

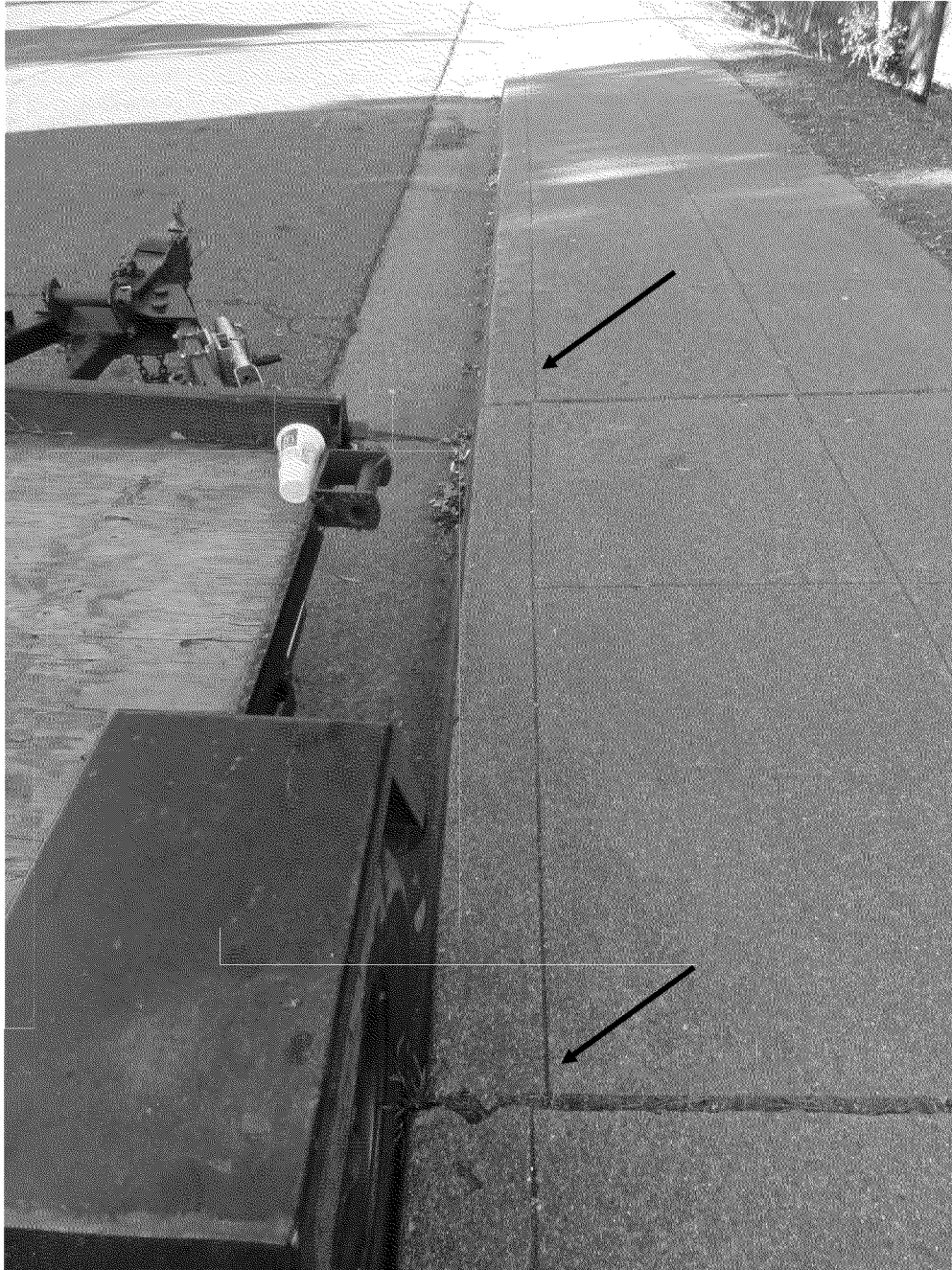


Figure 33. View southwestward along northwestern curb of Redacted. Arrows indicate two of three joints that exhibited right-lateral displacement. Photograph by Exponent, December 26, 2013.

East Bay Municipal Utility District Information

Other subsurface utilities are present in the vicinity of the Site. These include EBMUD water pipelines. PG&E and Exponent contacted EBMUD. Reportedly, EBMUD has experienced numerous pipe failures near the intersection of [Redacted] over the years. The recurrent water pipe failures in the vicinity of the Site have reportedly occurred approximately every ten years. EBMUD has identified the cause of the failures as ground movement resulting from Hayward Fault movement and/or landslides. Exponent understands the EBMUD pipelines that have experienced recurrent failures are located north of the Site, on the northeast end of the retaining wall. The retaining wall is located on the toe of a landslide and within the likely zone of fault creep deformation.

EBMUD has reportedly designed and is in the process of installing flexible joints in their pipelines near the Site. These flexible systems are intended to “minimize pipeline directional changes and cross the fault line in a direction that ensures tension in the pipe instead of compression.”⁷

Creep Monitoring

Figure 28 shows the location of a creep monitoring station (alinement array) next to the freeway. This station [Redacted] Station) is located approximate [Redacted] of the Site. This station is currently being monitored annually by San Francisco State University with theodolite surveys of the alinement array.⁸ The USGS also monitors creep in the vicinity of the site, at the [Redacted]. This station is located approximately 3,900 feet southeast of the Site (i [Redacted]). The [Redacted] Station is currently being monitored every 10 minutes by an installed creepmeter.⁹ Additional details of the creep monitoring stations are included in Appendix D.

Based on information from the monitoring stations, the width of the creeping zone in the vicinity of the Site is likely 30 meters or less. This is consistent with conclusions from Lienkaemper (2006, revised 2008), who noted that “detailed mapping and surveying of creep evidence show that the deformation zone of the main creeping trace is as much as 20-m wide.”¹⁰

For the [Redacted], McFarland et al. (2009, revised 2013)¹¹ published creep data that have been recorded since 1989. For the [Redacted] the USGS published creep data that have been recorded since 1996. Figure 34 shows the available data for these two stations. As shown in this figure, at the [Redacted] Station a total displacement of

⁷ PG&E notes from phone conversation with EBMUD’s representative. Phone call on December 16, 2013.

⁸ McFarland, F. S., Lienkaemper, J. J. and Caskey, S. J. (2009, revised 2013). Data from Theodolite Measurements of Creep Rates on San Francisco Bay Region Faults, California, 1979-2012. USGS Open-File Report 2009–1119, v. 1.4. <http://pubs.usgs.gov/of/2009/1119/>.

⁹ <http://earthquake.usgs.gov/monitoring/deformation/data/download/table.php>.

¹⁰ Lienkaemper, J.J., 2006, revised 2008, Digital database of recently active traces of the Hayward Fault, California: USGS DS-177, <http://pubs.usgs.gov/ds/2006/177/>.

¹¹ McFarland, F. S., Lienkaemper, J. J. and Caskey, S. J. (2009, revised 2013). Data from Theodolite Measurements of Creep Rates on San Francisco Bay Region Faults, California, 1979-2012. USGS Open-File Report 2009–1119, v. 1.4. <http://pubs.usgs.gov/of/2009/1119/>.

over 76 mm has been measured since 1989, for an average creep rate of 3.2 mm/yr. At the [Redacted] Station a total displacement of over 57 mm has been measured since 1996, for an average creep rate of 3.3 mm/yr. The figure shows an acceleration of creep movement measured at the [Redacted] Station starting in approximately August 2013. The timing of the gas release event may be related to this acceleration of creep movement. Additional creep data information is included in Appendix D.

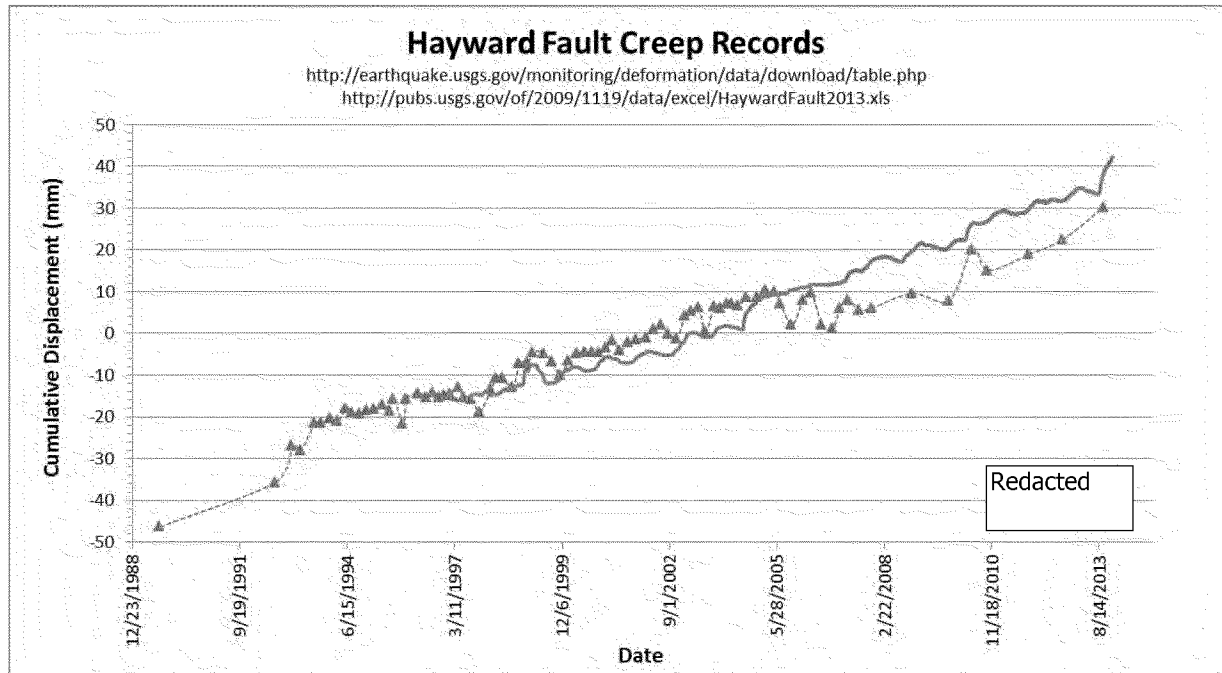


Figure 34. Hayward Fault creep records in the vicinity of [Redacted] (for available record interval). [Redacted]

Summary of Hayward Fault Location and Creep at Site

The Site is located within the Hayward Fault Zone as shown on geologic maps published by various agencies including the United States Geological Survey (USGS, see Appendix C), as designated by the State of California Alquist-Priolo Earthquake Fault Zones Act, and as interpreted by Exponent from aerial photographs and topographic maps. The Site also lies within a narrower zone in which the actively creeping fault trace has been mapped by the USGS (see Figure 28 and Figure 29). Possible surface evidence of creep in the form of right-lateral displacements in a retaining wall and reported damage to EBMUD water pipelines are also located within this narrow zone. Thus, the ground at the Site is subject to ongoing fault creep.

Fault-creep data recorded in the vicinity of the Site indicate that an average fault creep rate of 3.2 to 3.3 mm/yr has occurred since 1989. The amount of fault creep measured at the [Redacted] [Redacted] is 76 mm (since 1989) and 57 mm (since 1996), respectively.

Based on these data, the projected amount of fault-creep movement near the Site since 1987 (reported date of replacement of the northwest portion of the [Redacted] pipe, and likely

elbow stress relief) is approximately 80 to 85 mm over the width of the fault creep deformation zone. As previously noted, the exact width of fault deformation zone at the Site is uncertain, but likely less than 20 m.

Recent Seismic Activity

Figure 35 shows the recorded seismic events that occurred in the vicinity of the Site between August 1, 2013 and December 10, 2013. No significant events were recorded within a 50 km radius from the Site.¹² The closest event to the Site was a magnitude 2.0 earthquake approximately 3.5 miles southeast of the Site. The largest event was a magnitude 3.3 earthquake more than 10 miles east of the Site. Ground motions from these events did not cause significant loading of the pipe system at the Site.



Figure 35. Earthquakes within a 50-km radius from Site, and magnitude greater than 2.0, recorded between August 1, 2013 and December 10, 2013. Source: USGS: <http://earthquake.usgs.gov/earthquakes/map/>

Non-Seismic Ground Settlement

Exponent assessed the likelihood of ground settlement causing external forces on the pipe at the Site. Exponent considers it unlikely that ground settlement following the 1987 pipe replacement has been significant at the Site. This is supported by lack of evidence of significant ground settlement observed at the Site.

¹² Data obtained from USGS: <http://earthquake.usgs.gov/earthquakes/map/>.

In addition, as discussed in the Stress Analysis section of this report, the observed rupture mechanism was consistent with movement in a horizontal plane. Ground settlement includes a large vertical component. Therefore, Exponent concludes that overstress of the pipe at the failure location was not caused by ground settlement.

Landslide Movement

Exponent assessed the likelihood of landslide movement causing external forces on the pipe at the Site. As shown in Figure 36, the Site is located on the edge of a large ancient landslide. Exponent observed evidence of this landslide on topographic maps, aerial photographs, and in the field. In addition, a steep slope below Redacted is potentially susceptible to landsliding.



Figure 36. Map showing geomorphic and tonal features along recently active traces of the Hayward Fault. Based on 1939 (pre-development) aerial photographs. Source: California Division of Mines and Geology (now California Geological Survey), 1980, Fault Evaluation Report FER-102, Hayward fault (Oakland segment), Figure 4. Geomorphic and tonal features along recently-active traces of the Hayward fault, scale 1:24,000.

The large landslide occurred long before development of the neighborhood. Its boundary in the immediate vicinity of the Site is based on maps made by interpretation of aerial photographs taken in 1939.¹³ Subsequent grading for construction of [Redacted] included excavation of a portion of the landslide mass northwest of the Site, changing the loads acting on the Site slope, likely reducing the potential for sliding at the Site.¹⁴

The steep slope below [Redacted] has long been developed with houses. Exponent's review of geologic and geotechnical reports in the Land Stability files at the City of Oakland Building Services Division revealed no records of landslide activity at or below the Site.

Landslide movement typically occurs during or shortly after periods of wet weather or the occurrence of significant water pipe leaks. The gas release occurred after two years of below-normal rainfall, and EBMUD staff did not report any recent water main leaks near the Site during phone conversations with PG&E and Exponent.¹⁵

Exponent did not observe any evidence of active landsliding at the Site during our reconnaissance site visits.

Finally, as discussed in the Stress Analysis section of the report, the observed rupture mechanism was consistent with movement in a horizontal plane. Ground movement produced by landsliding toward the downslope side of [Redacted] would have resulted in a significant vertical displacement component. Therefore, Exponent concludes that it is unlikely that overstress of the pipe at the failure location was caused by landsliding toward the downslope side of [Redacted]

Exponent concludes that it is unlikely that overstress of the pipe at the failure location was caused by landsliding.

¹³ California Division of Mines and Geology (now California Geological Survey), 1980, Fault Evaluation Report FER-102, Hayward fault (Oakland segment), Figure 4, scale 1:24,000.

¹⁴ Potential sliding with a landslide toe at the excavation on the north side of [Redacted] is unlikely to cause significant ground movement at the Site. As described previously, repeated EBMUD water main breaks across [Redacted] from the Site have been attributed to either fault creep or landslide movement.

¹⁵ PG&E notes from phone conversation with EBMUD's representative. Phone call on December 16, 2013. Exponent's phone call with EBMUD on December 18, 2013.

Stress Analysis

The Abaqus finite element software package was utilized to create a finite element model of the region near the incident to investigate loading scenarios that might have contributed to the subject elbow fracture. The region modeled is shown in Figure 37. Lines from three different utilities were included in the model: a network of gas distribution lines, a sewer line, and a hydrant water line. Surrounding soil was also included in the model, but is not shown in the figure.

The model encompasses a region that is 14 feet by 14 feet, 12 feet deep, and centered near the fractured elbow. The geometry of the gas piping shown to the left of the elbow in the figure was created from measurements of the pieces extracted after the repair. The tee to the right of the elbow was assumed to be identical to the one on the left (i.e. the one extracted after the repair). The gas lines traveling towards [Redacted] and up and down [Redacted] were assumed to have nominal dimensions (three and four-inches respectively). The hydrant water line was assumed to be a six-inch Schedule 40 steel pipe filled with water. The sewer line was assumed to be an empty eight-inch PVC pipe. The gas lines were assumed to be pressurized to 54 psig.

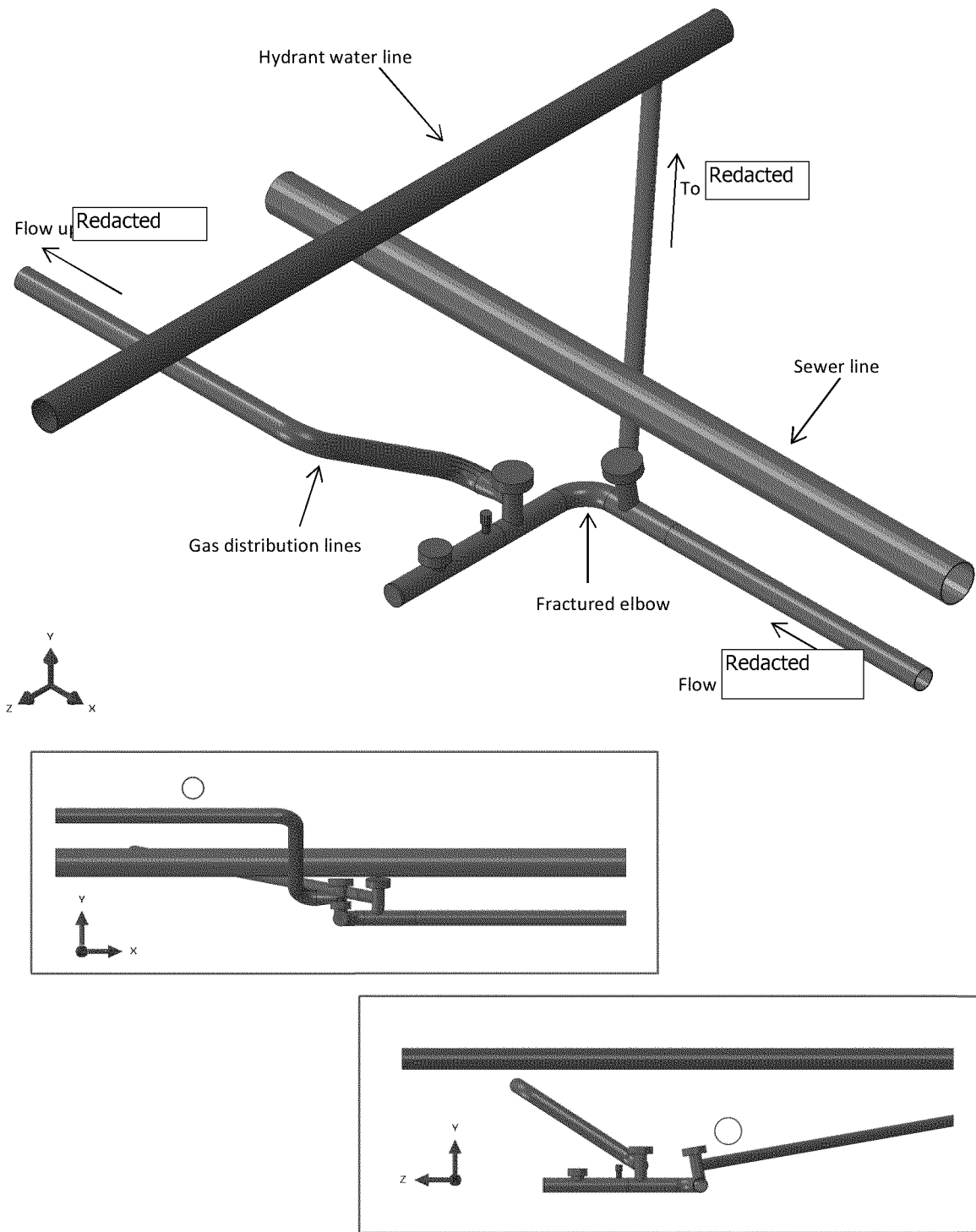


Figure 37. Network of pipes included in the finite element analysis. Surrounding soil was also included, but is not shown in the figure. The model encompasses a region that is 14 feet by 14 feet, 12 feet deep, and centered near the fractured elbow.

The finite element mesh used for the soil and pipes is shown in Figure 38. The subject elbow, the immediately adjacent pipes, the flange tees, and the soil were modeled with 3D hexahedral elements. The remaining gas pipes, the hydrant line, and the sewer line were all modeled with 3D continuum shell elements to reduce the numerical complexity. Approximately 560,000 elements were utilized in the model.

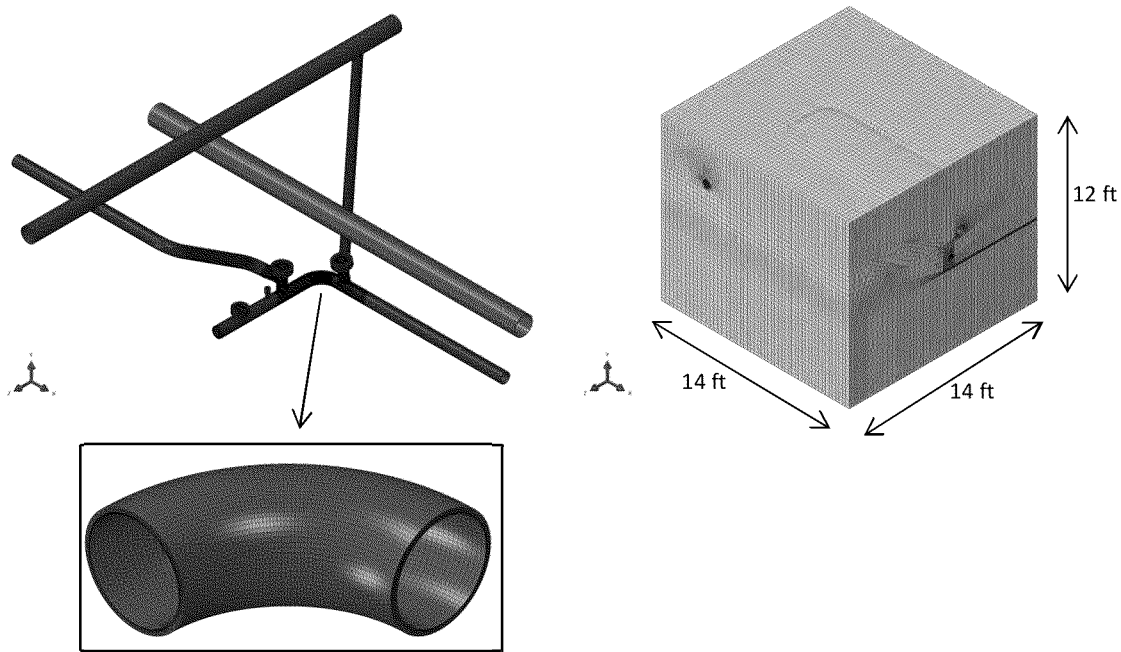


Figure 38. Mesh used in the finite element analysis. The failed elbow is shown in the lower left. The soil is shown in the upper right.

All materials used in the model were assumed to be elastic and are summarized in Table 4. Of all the materials utilized in the analysis, the soil properties produce the greatest uncertainty in the results. No soil samples from the trench material were obtained or tested. From evaluations of photographs taken during the pipe repairs, Exponent determined that the pipe trench material consisted of sand fill. Sand fill material is consistent with backfill material observed by Exponent in PG&E pipe trenches excavated during repairs of adjacent pipelines. The sand backfill material properties were modeled using typical values for sands (values between parentheses include sensitivity range evaluated in model).¹⁶ The range of material properties was selected to cover conditions for which the sand fill may have been medium dense (lower range of modeled parameters) to very dense (upper range of modeled parameters). The finite element analyses showed limited influence of the fill material properties in the results, and thus, no additional tests or refinements to these parameters were considered necessary.

¹⁶ Kulhawy, F.H. and Mayne, P.W. (1990). Manual on estimating soil properties for foundation design. Report EL-6800, Electric Power Research Institute, Palo Alto.

Table 4. Material properties used in the finite element model (numbers in parentheses indicate sensitivity range evaluated in the model).

Material	Density	Young's Modulus	Poisson's Ratio
Soil	120 pcf	500 atm (200 atm, 1000 atm)	0.3
Steel	0.285 pci	29,000 ksi	0.29
PVC	0.05 pci	440 ksi	0.41
Water	62.4 pcf	-	-

The contact interfaces between the gas lines and the soil were free to slide with a friction coefficient of 0.2. The sensitivity to this parameter has not been investigated, but the ability of the gas lines to slide with respect to their surrounding soil is expected to have an effect on the local stresses in the gas line.

Gravitational Loading

The first step of the model consists of applying gravity loading. The soil base was fixed in the vertical direction, and the four walls of the soil were fixed in the normal directions. The utility lines that intersect the model boundaries were constrained only by the surrounding soil and not by additional boundary conditions, so they may slide in or out of the soil walls. The top surface of the soil was coincident with the ground surface, so no loads or boundary conditions were applied to it. A uniform gravity load of 386 in/s² was applied to all elements, and the model was allowed to achieve geostatic equilibrium. The resulting tensile stresses in the pipe network and the incident elbow are shown in Figure 39 and Figure 40, respectively. Stresses were calculated to be less than 2 ksi for most of the network, with small localized regions as high as 4.4 ksi. The largest tensile stresses in the elbow were approximately 1.4 ksi; roughly one-fiftieth of the measured elbow tensile strength.

One uncertainty in the model geometry was the vertical distance between the water line and the gas line and the support condition beneath the water line near the gas line. It is possible that the water line was resting directly on the gas line and was not fully supported by soil in this vicinity. To determine the sensitivity of the stresses in the subject elbow to the water line support condition, a second model was built such that six feet of the water line in the vicinity of the gas line was unsupported by soil. For this condition, a larger load from the water line is transferred directly to the gas line. The tensile stresses calculated in the incident elbow are shown in the lower half of Figure 40; the largest tensile stresses were approximately 1.5 ksi, which was only slightly larger than the nominal condition and not large enough to cause failure. Thus, the support condition of the water line in the vicinity of the gas line was determined to have a negligible contribution to the failure.

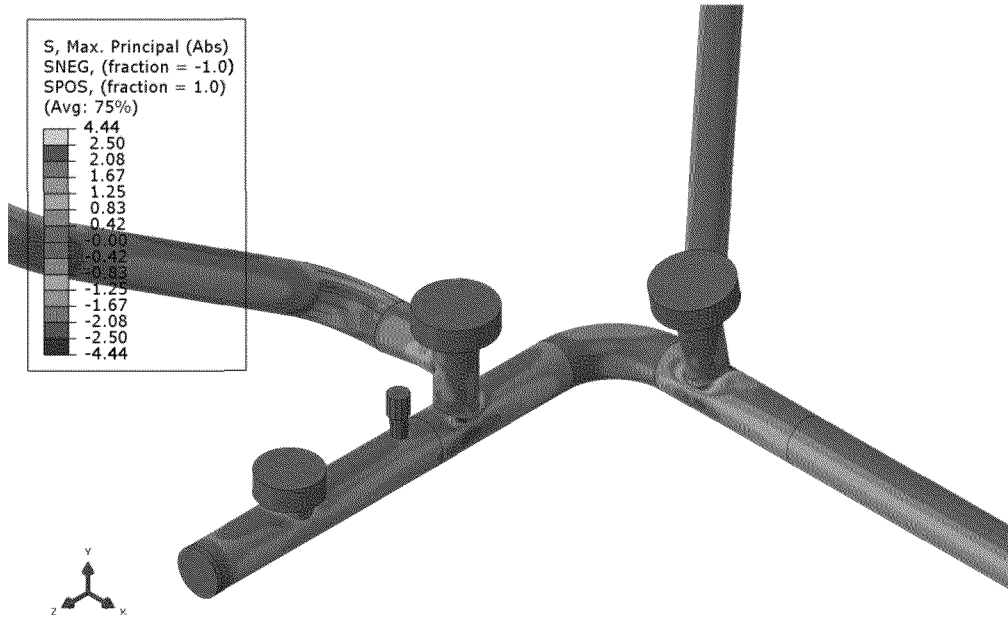


Figure 39. Tensile stresses in the pipe network subjected to gravitational loading. Units are ksi.

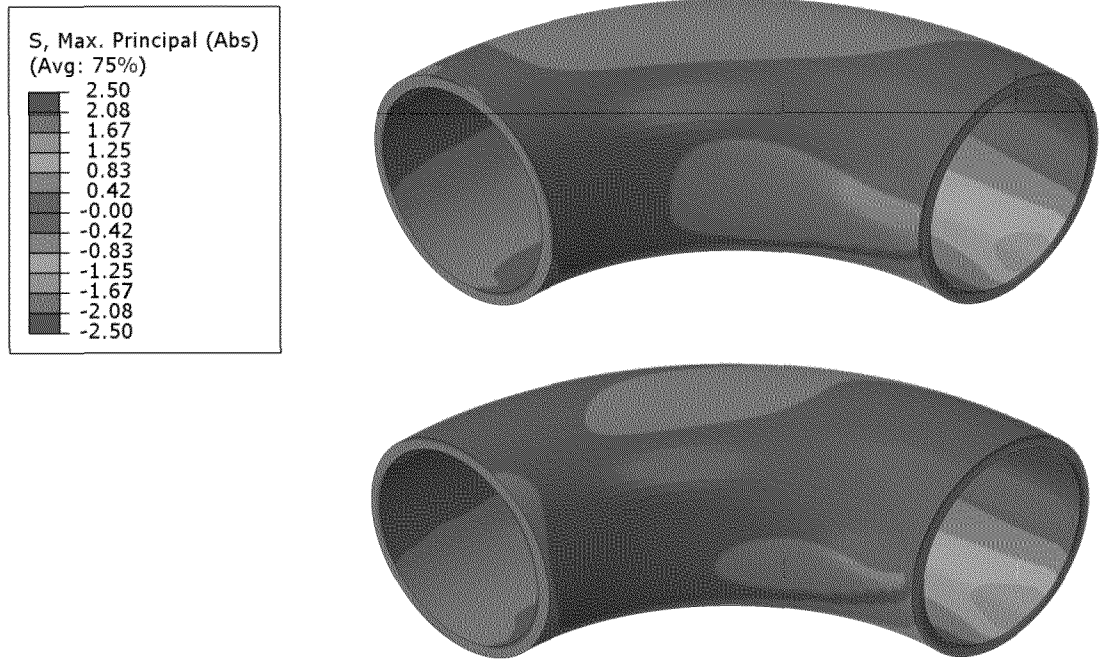


Figure 40. Tensile stresses in the incident elbow subjected to gravitational loading with nominal water pipe support (top) and 6 ft unsupported water pipe (below). Units are ksi.

In order to determine the sensitivity of the elbow stresses to loading from heavy equipment on the road-surface, a load of 80,000 lbf was applied to the surface of the soil directly above the incident elbow in a patch of approximately 9” by 10”. This is approximately equivalent to a tractor trailer loaded to the legal limit, but carrying that load on just one tire instead of distributing the load over many tires.^{17,18} The resulting tensile stresses in the elbow are shown in Figure 41. The peak tensile stress is approximately 4.5 ksi and is located on the lower surface of the inside of the elbow. Tensile stresses near the failure location are approximately 2 ksi; this is not a sufficient amount of stress to cause failure.

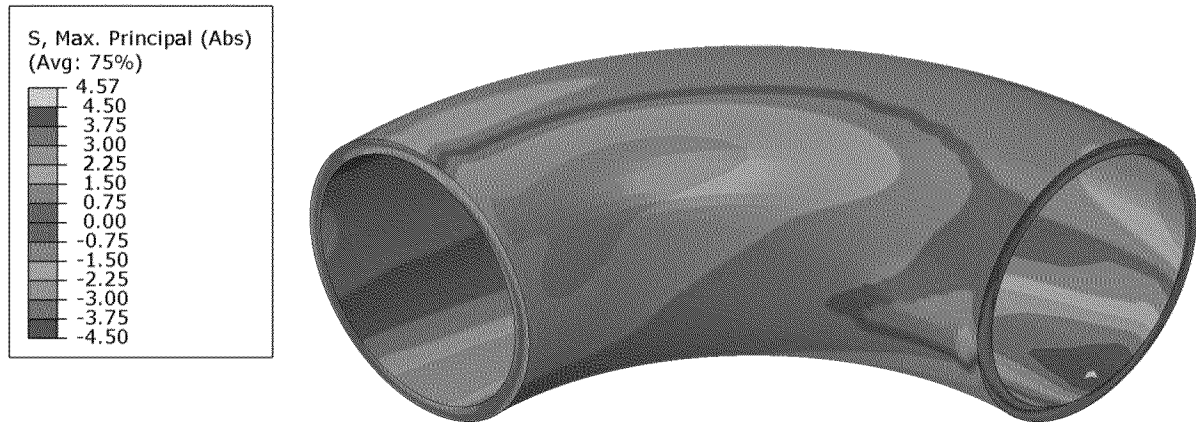


Figure 41. Tensile stresses in the elbow when subjected to an 80,000 lbf truck load on the surface of the soil above the elbow.

Ground Movement Shearing

Because gravitational loading alone is not sufficient to achieve tensile stresses in the elbow that are consistent with the observed mode of failure, ground shearing movement was investigated as a possible source of stresses. After the model achieved equilibrium with gravitational loading, the soil was sheared in the horizontal plane to simulate ground movement associated with right-lateral strike-slip creep of the Hayward Fault or to simulate possible ground movement due to the ancient landslide. These two shearing directions are diagrammed in Figure 42. Two additional shearing directions were considered to investigate the sensitivity of the fault shearing direction; these directions were rotated $\pm 10^\circ$ from the fault creep nominal condition shown in Figure 42.

¹⁷ U.S. Code Title 23 Section 127: Vehicle weight limitations – Interstate System

¹⁸ P. Yap, “Truck Tire Types and Road Contact Pressures,” Second International Symposium on Heavy Vehicle Weights and Dimensions. Kelowna, Canada. June, 1989.

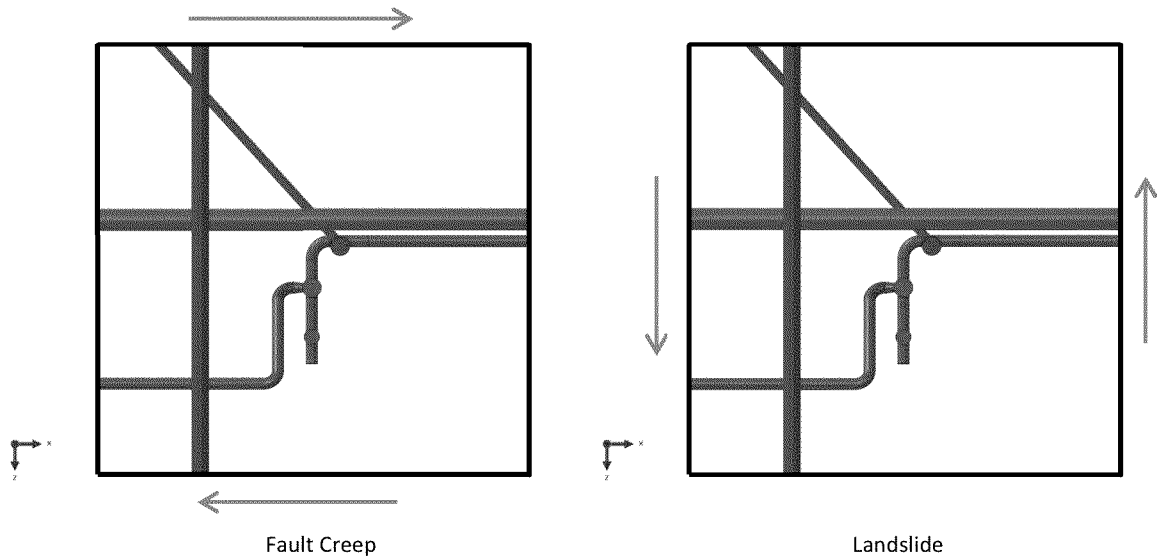


Figure 42. The two primary ground movement shearing directions considered in the finite element model. The left image shows the shearing consistent with right-lateral strike-slip creep of the Hayward Fault, and the right image shows the shearing consistent with ground movement due to a nearby landslide.

To allow for arbitrary shearing directions that might not correlate with the walls of the model (e.g. the perturbation directions for the fault creep), the shearing of the soil boundaries was achieved by using a global model / submodel configuration. The global model was a simple block of soil slightly larger than the model which contains the pipe network (this detailed model with the pipes is now referred to as the submodel). The global model is shown in Figure 43. The model was meshed with approximately 130,000 3D hexahedral elements. The global model can be easily rotated and sheared in a desired direction, and the soil walls of the submodel will then follow the resulting displacements from the global model without any modifications to the submodel geometry or mesh. This is demonstrated schematically for the fault-creep condition in Figure 44. For all models, four inches of shear was applied to the 20 foot-wide global model, which results in a gradient of 0.2 inch per foot of model width, or 2.8 inches (~71 mm) of shear for the 14-foot wide submodel; this applied shear is consistent with creep deformation data of the Hayward Fault in the vicinity of the site.¹⁹

¹⁹ As previously discussed, based on the creep monitoring data, the projected amount of fault creep movement near the Site since 1987 (reported date of replacement of the [Redacted] pipe, and likely elbow stress relief) is approximately 80 to 85 mm over the width of the fault creep deformation zone. The exact width of fault deformation zone at the Site is uncertain, but likely less than 20 meters. Because the finite element model represents only a portion of the entire fault deformation zone at the Site, modelling only a portion (71 mm) of the total projected creep (80 to 85 mm) is consistent with measured creep data.

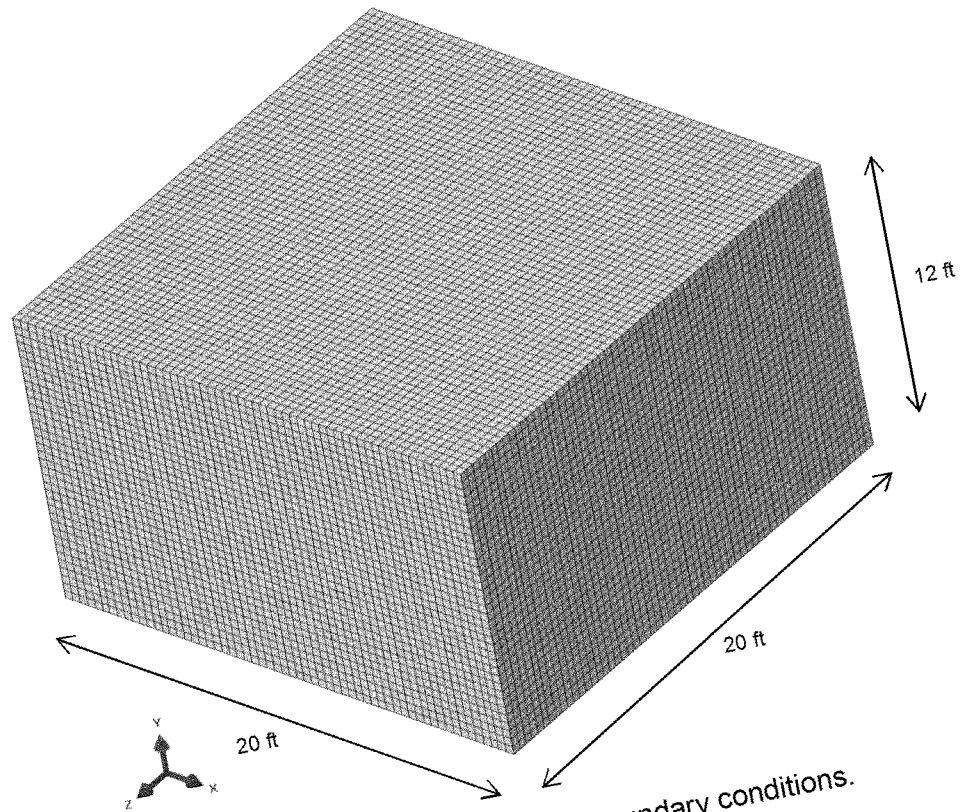


Figure 43. Global model used to apply shearing boundary conditions.

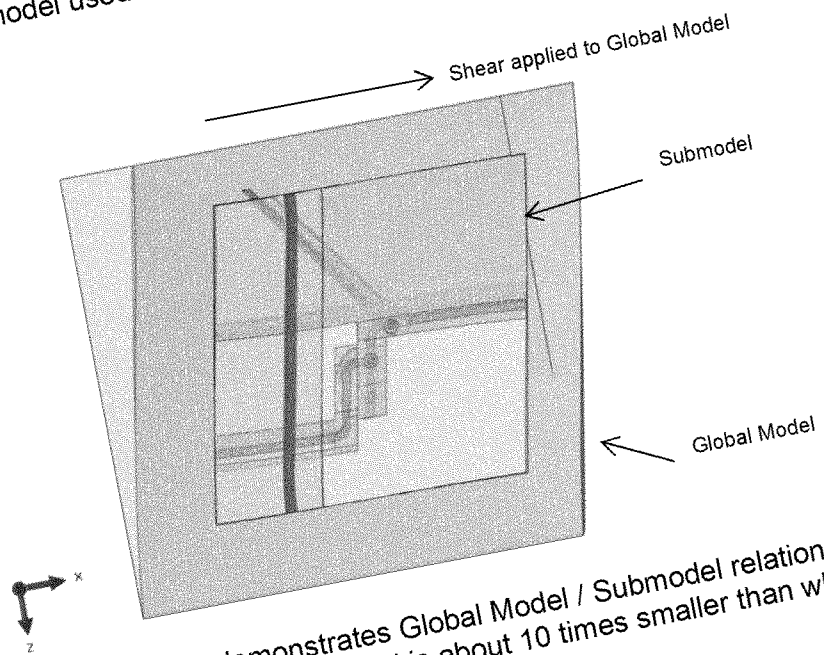


Figure 44. Schematic that demonstrates Global Model / Submodel relation. Actual shearing applied in model is about 10 times smaller than what is shown here.

The resulting deflections of the gas pipe network when subjected to 0.2 in/ft of horizontal shear in the fault creep and landslide directions are shown in Figure 45. Tensile stresses in the gas lines in the vicinity of the incident elbow are shown in Figure 46. In both shearing conditions, tensile stresses were concentrated in the incident elbow near the failure location, i.e. on the outside surface of the elbow intrados, and have nearly the same tensile stresses for the same amount of ground shearing. The peak tensile stresses on the outside surface of the elbow intrados are 49.1 ksi for both the fault creep and landslide cases, and are shown on the left side of Figure 47. This stress approaches the magnitudes necessary to cause failure. However, note that the peak elbow stress occurred on the lower inside surface of the elbow, as indicated by the gray region in the left images of Figure 47, not on the outside wall of the elbow intrados. This point will be revisited later. Nonetheless, the magnitude, location and direction of peak tensile stress on the outside wall of the elbow intrados were consistent with the fractured incident elbow. Plots of the tensile stress direction on the outside surface of the elbow for the fault-creep and landslide-shear cases are shown on the right side of Figure 47.

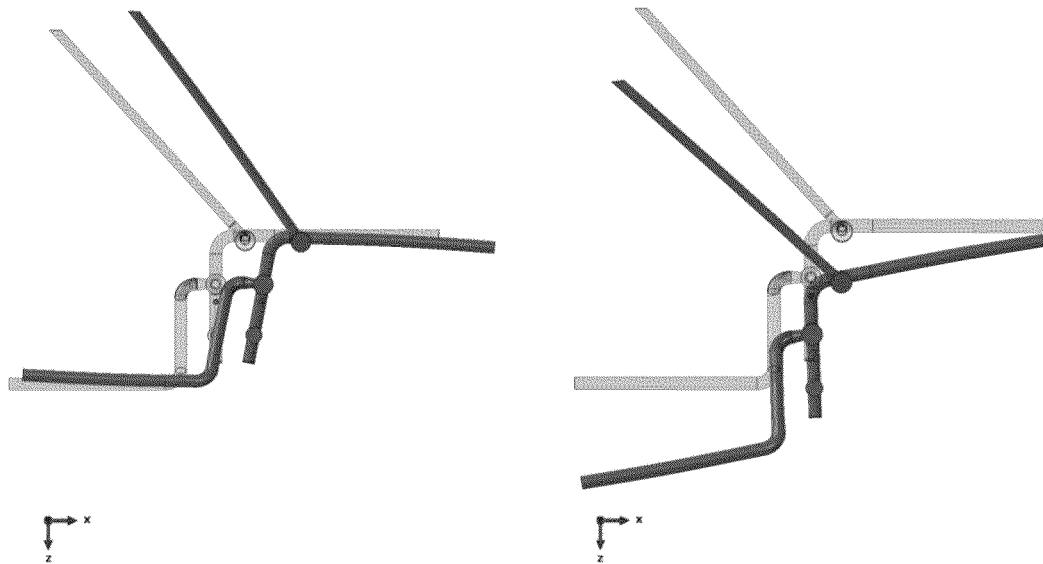


Figure 45. Deformed shapes of the gas pipe network when subjected to fault-creep shear (left) and landslide shear (right). The total shearing applied is 0.2 in/ft, but the deformations are scaled by a factor of 10.

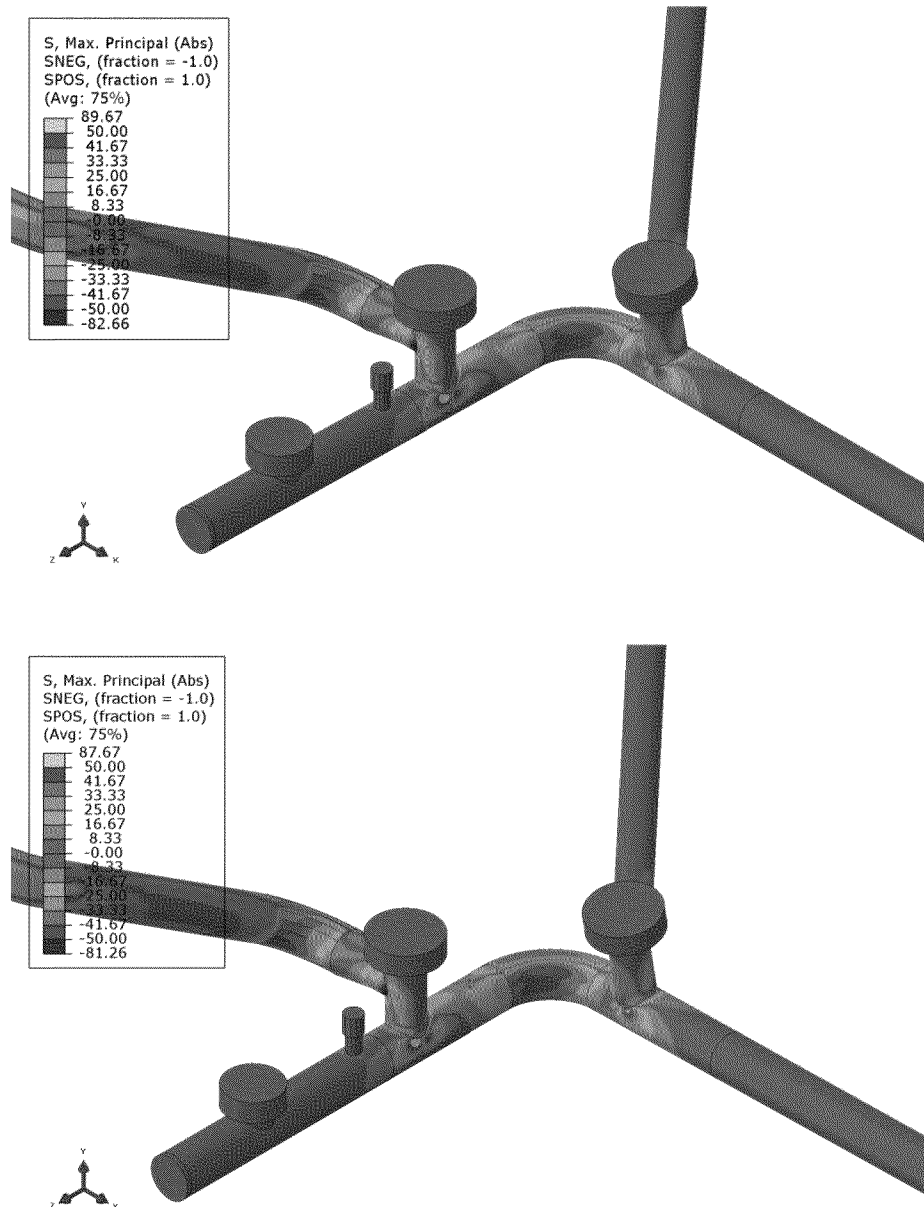


Figure 46. Tensile stresses in the gas pipes when subjected to 0.2 in/ft of shear in the fault creep direction (top) and the landslide shear direction (bottom). Units are ksi.

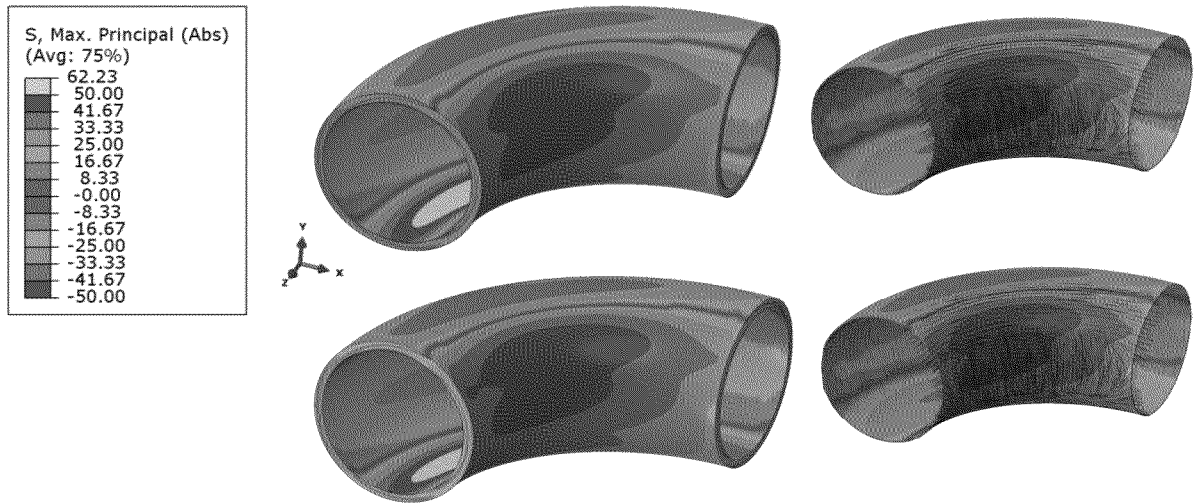


Figure 47. Tensile stress contours of the incident elbows subjected to shearing in the fault-creep direction (top) and the landslide direction (bottom). Images on the right show tensile stress directions for the outside wall of the elbow. The location and direction of the peak tensile stresses on the elbow exterior are consistent with the crack opening direction observed in the failed elbow. Units are ksi.

To further investigate the sensitivity to shearing direction on the peak tensile stress magnitude and location, the fault creep shearing direction was varied by $\pm 10^\circ$. Tensile stresses in the gas lines in the vicinity of the incident elbow are shown in Figure 48. The peak tensile stresses on the outside wall of the elbow intrados were slightly higher for the $+10^\circ$ shearing direction and lower for the -10° direction (50.2 ksi and 42.7 ksi respectively) as compared with the nominal fault creep condition in Figure 46. The location of the peak stress also shifted along the axial position of the elbow.

To investigate the sensitivity of soil modulus on the peak tensile stress magnitude, two other soil moduli were investigated, 200 atm and 1000 atm, as compared with the nominal value of 500 atm. Tensile stresses in the gas lines in the vicinity of the incident elbow are shown in Figure 49. The peak tensile stresses on the outside wall of the elbow intrados were 41.3 ksi and 55.2 ksi for the 200 atm and 1000 atm moduli soils, respectively. While the magnitude of stress varies for the different soil moduli, the location of the peak tensile stress on the outside wall of the elbow does not change. All of these stresses are summarized in Table 5, and all are approaching magnitudes that would be consistent with failure of the elbow.

Table 5. Summary of peak tensile stresses on the exterior of the incident elbow near where the failure was observed for different ground shearing movements.

Model	Peak Tensile Stress on Outside Wall of Elbow Intrados (ksi)
Fault Creep	49.1
Landslide	49.1
Fault Creep +10°	50.2
Fault Creep -10°	42.7
Fault Creep, 200 atm Modulus	41.3
Fault Creep, 1000 atm Modulus	55.2

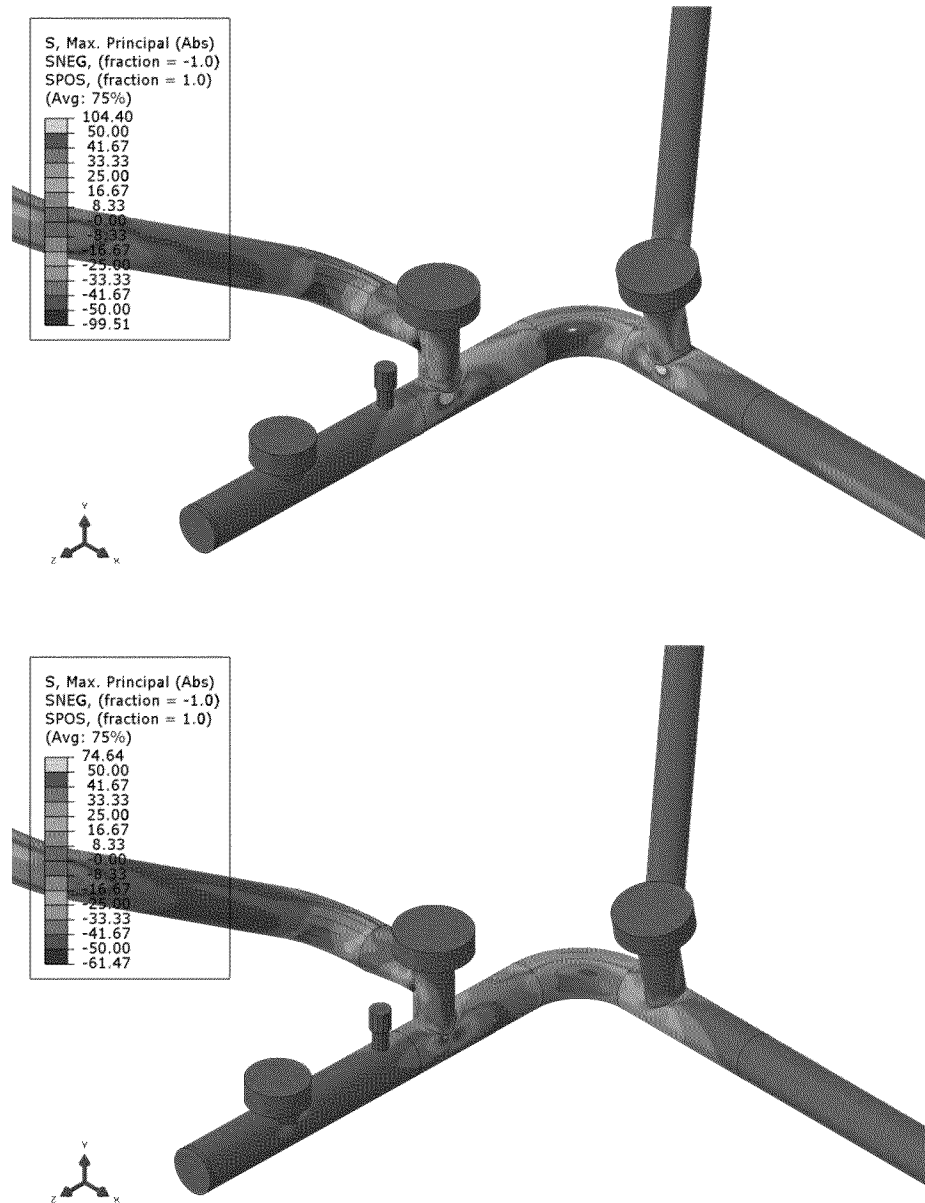


Figure 48. Tensile stresses in the gas pipes when subjected to 0.2 in/ft of shear in the fault creep +10° direction (top) and the fault creep -10° direction (bottom). Rotation angles are with respect to the model's y-axis. Units are ksi.

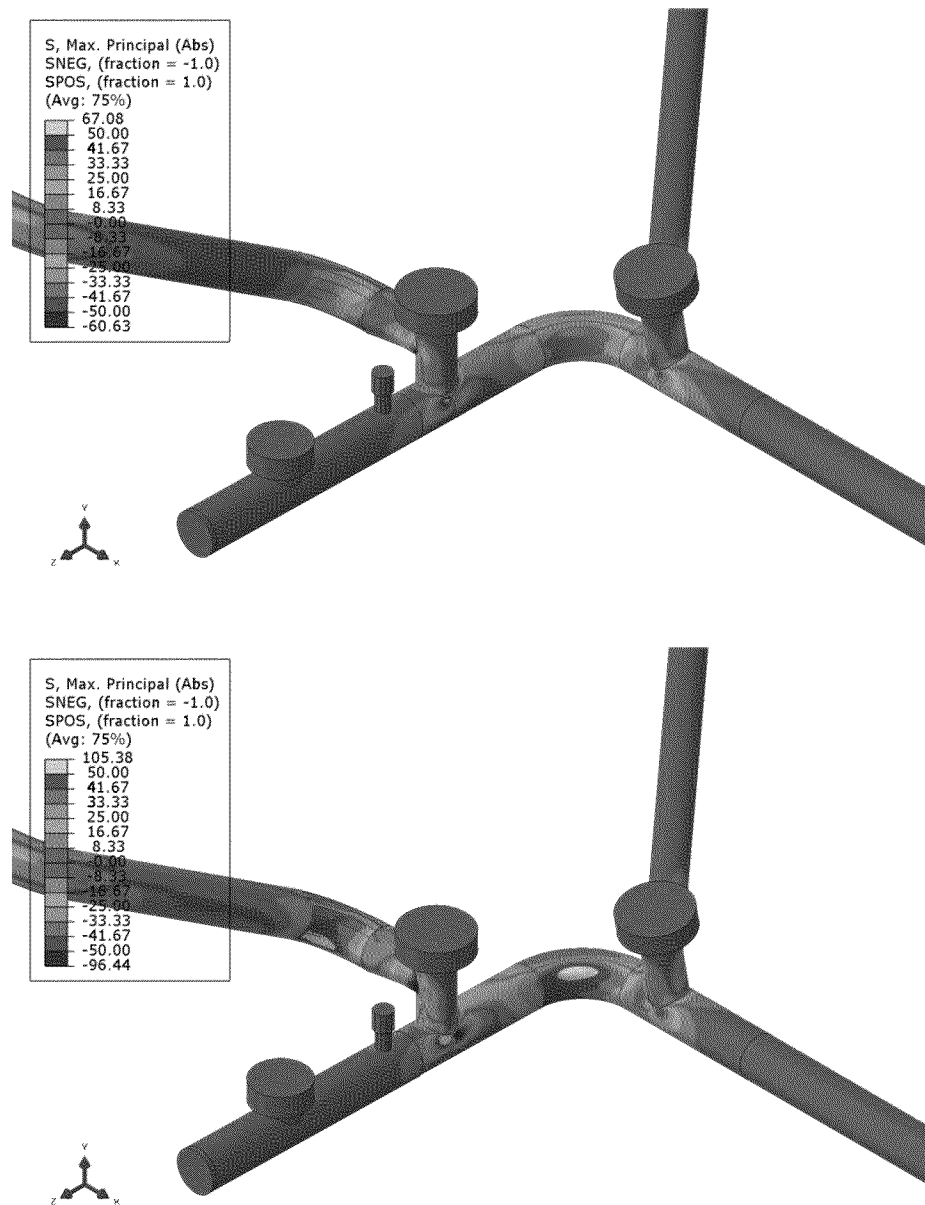


Figure 49. Tensile stresses in the gas pipes when subjected to 0.2 in/ft of shear in the fault creep direction but with varying soil moduli, 200 atm (top) and 1000 atm (bottom). Units are ksi.

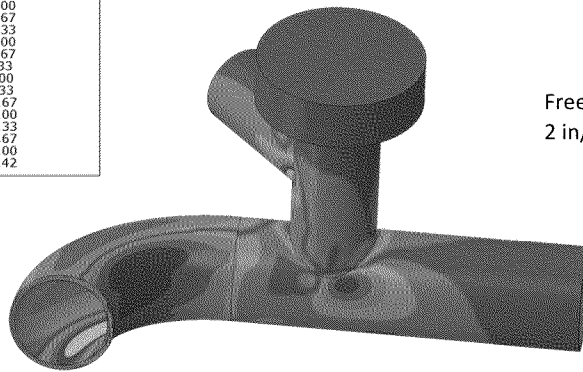
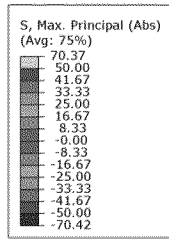
As noted earlier, the peak tensile stress in the incident elbow was located on the lower inside surface of the elbow, as indicated by the gray region in the upper left image of Figure 47. However, the location of the peak tensile stress is strongly dependent on the boundary condition at the end of the Redacted gas line. The model described thus far allows the pipe to slide unconstrained in the soil. However, the actual Redacted pipe is constrained axially by an elbow that is outside the bounds of the model. This elbow reacts against soil which would provide some axial constraint on the pipe; however, it is not a rigid constraint. To investigate this sensitivity, two additional models were constructed: one model used a rigid constraint on the

Redacted pipe such that it cannot move axially and is forced into compression during the shearing, and a second model which provided a softer constraint that allowed the pipe to move only half the distance that it would if it were free to slide. The resulting tensile stresses in the region of the elbow and neighboring tee are shown in Figure 50. In all cases, the tensile stresses are near the magnitude to cause failure.

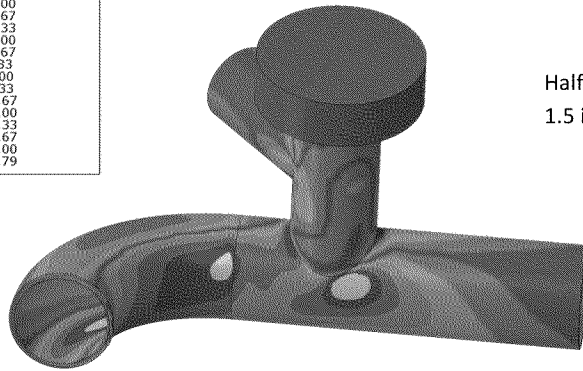
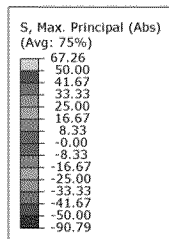
A summary of the peak tensile stress on the outside and inside walls of the elbow for the three boundary condition cases is presented in Table 6. It is important to note that decreasing levels of shear were applied to the models as the constraint was increased. The reduction in ground movement shearing reduces the stresses on the inside wall of the elbow. If the constraint on the end of the Redacted pipe were unchanged, then we would also expect the stress on the outside wall to be reduced in a constant ratio. However, the constraint on the end of the Redacted pipe causes the stress on the outside of the elbow (as well as the neighboring tee) to increase, and therefore causes the peak tensile stress location to switch from the lower inside surface to the outside surface of the elbow intrados. The fully constrained condition is unrealistic and causes very high stresses in the tee; the true constraint condition is likely somewhere between the two extremes of free and fixed.

Table 6. Peak tensile stresses in the incident elbow for different boundary conditions on the Redacted pipe (note that the models have decreasing amount of shear despite increasing stresses on the elbow outside wall).

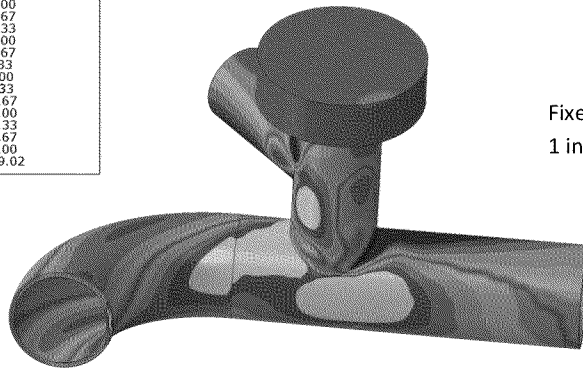
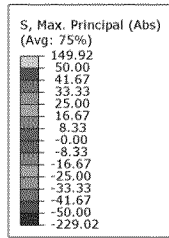
Model	Fault Creep Shear	Peak Tensile Stress on Elbow (ksi)		Ratio Inside/Outside Stress
		Inside Wall	Outside Wall	
No Axial Constraint (nominal)	2 in/ft	62.2	49.1	1.26
Half Constrained	1.5 in/ft	56.4	53.4	1.06
Fully Constrained	1 in/ft	51.9	66.5	0.78



Free Boundary Condition
2 in/ft fault creep shear



Half Constrained Boundary Condition
1.5 in/ft fault creep shear



Fixed Boundary Condition
1 in/ft fault creep shear

Figure 50. Tensile stresses in the incident elbow and neighboring tee for different boundary conditions on the Redacted pipe. Note that the models have decreasing amount of shear despite increasing stresses. Units are ksi.

Post-Failure Repair

A finite element model was created to investigate the current stresses in the incident area following removal of the subject elbow and downstream piping. This new model is shown in Figure 51. The model was subjected to fault-creep shear of 0.2 in/ft consistent with the shear modeled in the subject elbow analysis. Tensile stresses in the repaired gas line near the location of the fractured elbow are shown in Figure 52; the stresses are reduced as compared with the stresses in the original configuration before the incident (upper image of Figure 50). Local stresses in the vicinity of the flange tee were predicted to be near 30 ksi. Thus, even after the removal of the subject elbow and associated downstream piping, stresses at the junction between the [Redacted] piping could be as high as 30 ksi.

As in the earlier models, the stresses in the tee are highly dependent on the constraint of the [Redacted] pipe. The excavation likely allowed local displacement and relief of some bending and compressive stresses at the [Redacted] junction, but the rotational-induced stresses from fault-creep shear likely remains, consistent with the image shown in Figure 52. These stresses will increase with further creep of the Hayward fault at this location.

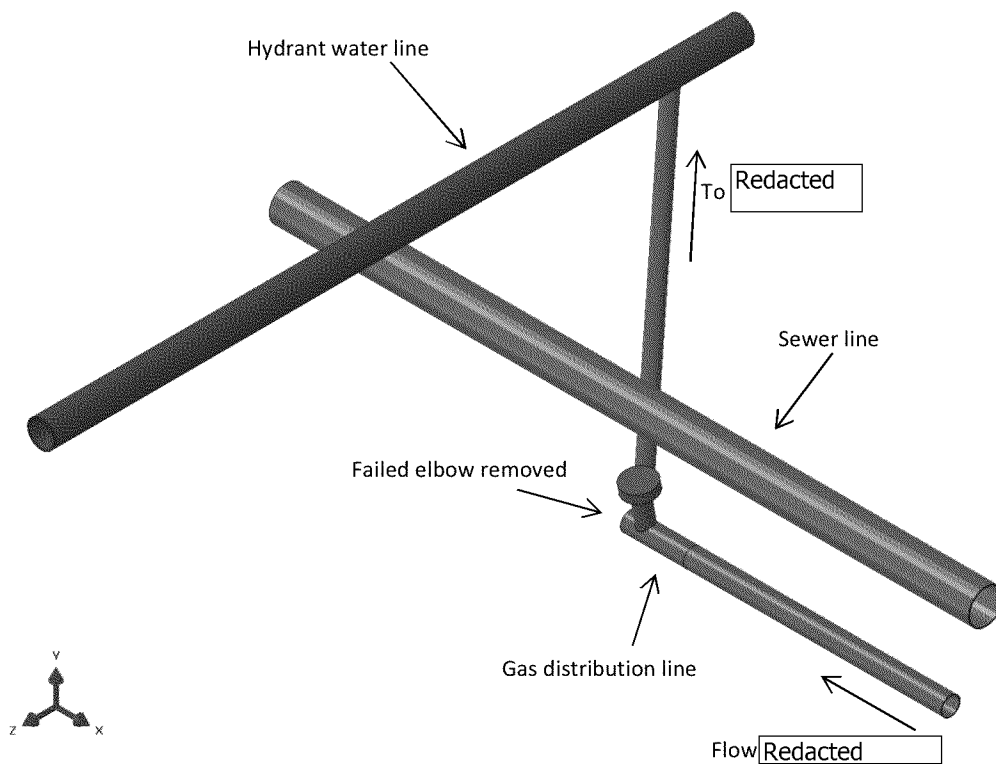


Figure 51. Post-repair model.

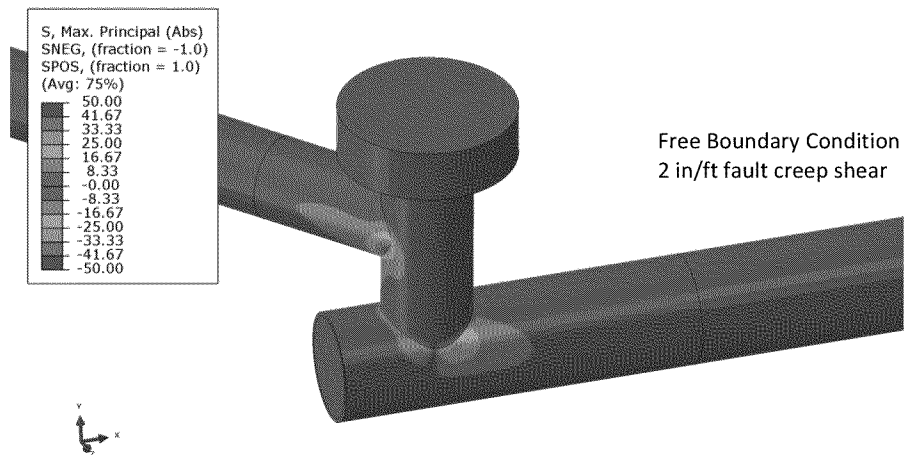


Figure 52. Tensile stresses after the post-failure repair in the flange tee neighboring the incident elbow for different boundary conditions on the [Redacted] pipe. Note that the models have decreasing amount of shear despite increasing stresses. Units are ksi.

Stress Analysis Discussion

Exponent's stress analysis indicated that the subject elbow likely fractured from stresses accumulated from creep along the Hayward Fault. Landslide shearing also produced stresses in the pipe network that are consistent with the failure location and failure mode; however, there was no observed or documented evidence of recent landsliding in the vicinity of the pipe failure. Perturbations in boundary conditions, soil material properties, and fault creep shear angle all changed the location and/or magnitude of the peak tensile stress in the elbow, but all cases still showed consistently high stresses near the failure location. Ground settlement and loading from heavy equipment on the road surface have been ruled out as potential contributors to the break because they do not produce stresses that are consistent with the failure location and failure mode.

Installation of the sanitary sewer line through a pipe bursting activity is unlikely to have contributed to the break. Recommended practices indicate that a line that is being burst should be at least two diameters away from neighboring utilities during pipe bursting activities²⁰. The sewer line is located less than eight inches from the [Redacted] gas line, which is less than two diameters (approximately 16 inches) away. However, the sewer line was rehabilitated in 2003, approximately ten years prior to the incident, and we would expect damage on neighboring utilities to occur during or shortly after the bursting event. Additionally, stresses incurred during pipe bursting are known to decrease with time²⁰. Thus, the pipe bursting activity likely did not significantly affect the stresses at the time of failure.

²⁰ J Simicevic & RL Sterling, Guidelines for Pipe Bursting, TTC Technical Report #2001.02, Prepared for U.S. Army Corps of Engineers, Engineering Research and Development Center (ERDC), March 2001.

After the failure, the connection between the [Redacted] pipe remains intact. Exponent's stress analysis indicates that local stresses at this connection may be approximately 30 ksi. As more fault creep occurs in the future, these stresses are expected to increase.

Post-Survey Observation of Repair Excavations

PG&E conducted a surface leak-detection survey of gas lines in the neighborhood surrounding the Site after the [Redacted] release occurred. PG&E developed a repair schedule prioritized by grade of leak, assigned repair crews, and asked Exponent geologic/geotechnical staff to observe the leaks and evaluate whether any were the result of ground movement. Exponent observed leak location and excavation by PG&E during the period December 17, 2013 through January 3, 2014. As shown in Table 7, Exponent observed fourteen excavations in which twelve leaks were detected and repaired. These included all of the Grade 1, 2+, and 2 leaks identified during the survey, and also several Grade 3 leaks.

Table 7. Post-Survey Gas Line Repair Excavations Observed by Exponent.

Address Closest to Excavation ²¹	Leak Present?
Redacted	Yes
	No
	No
	Yes
	Yes
	Yes
	Yes
	Yes
	Yes
	Yes
	Yes
	Yes
	Yes
	Yes

Nine of the leaks were in steel piping and were caused by corrosion. At two of these locations the corrosion was localized in a mechanical gouge on the pipe. Three of the leaks were in plastic piping. Two of these were at loose caps and one in a cracked fitting.

²¹ Exponent understands that PG&E records address where leak was first detected at surface. This table lists address closest to excavation in which leak was located and repaired.

Exponent observed no evidence that any of the leaks resulted from ground movement. In addition, we observed no indications of external load damage to the pipes exposed in the excavations.

Threat Category Assessment

The Pipeline and Hazardous Materials Safety Administration (PHMSA) indicates that pipeline operators must consider each of the eight threats listed below in Table 8 to their pipeline system. Based on our analysis presented above, the only threat that contributed to (or caused) the subject elbow fracture and the corresponding [Redacted] release is from natural forces: ground movement caused by creep along the Hayward Fault. All other threats have been determined to be unlikely contributors.

Table 8. Assessment of the contribution of each of the eight pipeline system threats to the [Redacted] event.

Threat Category	Conclusion
Corrosion	Unlikely
Natural Forces	Likely
Excavation Damage	Unlikely
Other Outside Forces	Unlikely
Material or Weld	Unlikely
Equipment Failure	Unlikely
Incorrect Operations	Unlikely
Other	Unlikely

Corrosion – While some evidence of corrosion was present on the subject elbow, no corrosion was observed along the fracture. Metallurgical analysis determined a corrosion-induced cracking mechanism such as stress corrosion cracking was not present.

Natural forces – As detailed above, the release location is located directly within a creeping zone of the Hayward Fault. Metallurgical and stress analyses indicated that the elbow fracture is consistent with overload fracture from ground-motion shear.

Excavation damage – No evidence of excavation damage was observed on the subject elbow.

Other outside forces – Other outside forces, such as from heavy equipment, has been ruled out as possible contributing causes through stress analysis. Sewer pipe slip-lining has been ruled

out as a possible contributing cause due to the extended time between sewer installation and the failure.

Material or weld – The elbow materials met the pertinent ASTM specifications. The break did not occur at or near a weld.

Equipment Failure – There is no evidence that any equipment failure could have caused the observed fracture in the subject elbow.

Incorrect Operations – There is no evidence that any incorrect operations contributed to the subject elbow fracture.

Other – There is no evidence that any failure mechanism other than creep of the Hayward Fault contributed to the subject elbow fracture.

Conclusions

Exponent conducted an investigation to help determine the cause of the PG&E distribution pipeline rupture that occurred near the intersection of [Redacted] in Oakland, California on December 10, 2013. Exponent's investigation included inspection of the leak site, historical review of PG&E's construction documents, a fire cause and origin study, metallurgical analysis, geotechnical analysis, analysis of other leak locations within the immediate area, and finite element-based stress analysis of the effect of ground movement on the subject elbow and associated piping. Our findings are listed below:

- The fractured elbow that resulted in the December 10, 2013 leak was part of a 1946 four-inch steel pipe installation. Historical PG&E work documents described work conducted at the leak site in 1946, 1965, and 1987. Our review of the as-built construction drawings shows that they are consistent with the features observed in the ground. The subject elbow was part of the 1946 installation, and was specified to be made from ASTM A 106 Grade A or Grade B material.
- Leaking natural gas was ignited on the ground/street surface directly above the broken elbow. Ignition from the various utilities in the area was ruled out. The most likely cause(s) of ignition were from a passing automobile, or by transient sources, such as a discarded cigarette.
- The subject elbow fractured because it was subjected to stresses higher than its tensile strength. The elbow fractured in a brittle manner, and no evidence of progressive cracking, such as fatigue or stress corrosion cracking (SCC) was observed. There were no manufacturing defects, mechanical damage, or wall thinning due to corrosion that contributed to the break. The pipe elbow met the appropriate standards for tensile properties and chemistry.
- The leak site is located within the Hayward Fault Zone, and also lies within a narrower zone containing an actively creeping fault trace. The leak site also lies within an ancient landslide area. Ground-movement shear, caused by creep along this section of the right-lateral strike-slip Hayward Fault, is the likely cause of the stresses that resulted in the elbow rupture. Other possible ground movement mechanisms - recent landslide movement, seismic activity, and settlement - were evaluated and determined to be unlikely to have significantly contributed to the elbow rupture. Exponent has also determined that stresses from heavy equipment road-surface loading as well as the apparent 2003 sewer-line rehabilitation are unlikely to have contributed to the elbow rupture.
- After the failure, the connection between the [Redacted] pipe remains intact. Exponent's stress analysis indicates that local stresses likely remain in the existing configuration. As more fault creep occurs in the future, these stresses are expected to increase. Exponent recommends the current connection be replaced to relieve the current stresses.

- Leaks found during surveys conducted after the December 10, 2013 rupture event in the local area were not caused by ground movement. Rather, the bulk of these leaks were attributed to local corrosion of steel pipe.

Appendix A

Anamet, Inc. Reports



LABORATORY CERTIFICATE

LABORATORY NUMBER: 2004-0017
 CUSTOMER AUTHORIZATION: Credit Card
 DATE SUBMITTED: December 13, 2013
 REPORT TO: Exponent
 Attn: Redacted
 149 Commonwealth Drive
 Menlo Park, CA 94025

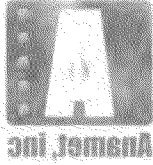
SUBJECT:
 One pipe elbow segment was submitted for chemical analysis and tensile testing. The sample was identified as 4" welded elbow segment with cracks in evidence, P/N 109032.

SPECTROCHEMICAL ANALYSIS
 (Reported as Wt. %)

Sample		4" Elbow
Aluminum	(Al)	0.01
Boron	(B)	<0.0003
Carbon	(C)	0.13
Chromium	(Cr)	0.01
Cobalt	(Co)	<0.002
Columbium	(Cb)	<0.002
Copper	(Cu)	0.02
Iron	(Fe)	Remainder*
Manganese	(Mn)	0.42
Molybdenum	(Mo)	<0.002
Nickel	(Ni)	0.02
Phosphorus	(P)	0.007
Silicon	(Si)	0.16
Sulfur	(S)	0.018
Titanium	(Ti)	<0.002
Vanadium	(V)	<0.002
Carbon Equivalent (C.E.) %		0.20

* Includes undetermined elements

28102 Eden Landing Road, Suite 3, Hayward, California 94542-3811 Phone: 510-887-8811 Fax: 510-887-8437
 This report shall not be reproduced, except in full, without the written approval of Anamet, Inc. ©2008 Anamet, Inc. All rights reserved.



LABORATORY CERTIFICATE

Lab. No. 2004-9717

TRANSVERSE TENSILE TEST:
(ASTM A370-10)

4" Elbow Segment, P/N 109032

Dimensions of Specimen (in.):	
Width	0.259
Thickness	0.218
Area (in ²)	0.0228
Tensile Strength (psi)	75600
Yield Strength 0.2% Offset (psi)	62600
Yield Strength 0.2% E.U.L. (psi)	N/A*
Elongation in 1" Gage (%)	19

* Specimen bending due to curvature

This testing was completed on December 17, 2013 and performed in accordance with the customer's authorization.

Submitted by:

Redacted

Redacted
Quality Manager

27



LABORATORY CERTIFICATE

REPORT TO: [Redacted]
 DATE SUBMITTED: December 17, 2013
 CUSTOMER AUTHORIZATION: Credit Card
 LABORATORY NUMBER: 2004.9717A
 December 19, 2013
 Attn: [Redacted]
 149 Commonwealth Drive
 Menlo Park, CA 94025

SUBJECT:

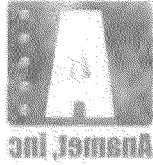
12/17/2013. The sample was identified as 4" line straight section, P/N 109241. One pipe straight segment was submitted for chemical analysis and tensile testing on

SPECTROCHEMICAL ANALYSIS
 (Reported as Wt. %)

Sample		4" Pipe
Aluminum	(Al)	<0.002
Boron	(B)	0.0003
Carbon	(C)	0.27
Chromium	(Cr)	0.04
Cobalt	(Co)	<0.01
Columbium	(Cb)	<0.002
Copper	(Cu)	0.07
Iron	(Fe)	Remainder*
Manganese	(Mn)	0.63
Molybdenum	(Mo)	0.01
Nickel	(Ni)	0.08
Phosphorus	(P)	0.011
Silicon	(Si)	<0.002
Sulfur	(S)	0.024
Titanium	(Ti)	<0.002
Vanadium	(V)	<0.002
Carbon Equivalent (C.E.) %		0.40

* Includes undetermined elements

26102 Eden Landing Road, Suite 3, Hayward, California 94543-3811 Phone: 510-887-8811 Fax: 510-887-8427
 This report shall not be reproduced, except in full, without the written approval of Anamet, Inc. ©2008 Anamet, Inc. All rights reserved.



LABORATORY CERTIFICATE

Lab. No. 5004-9717A

TRANSVERSE TENSILE TEST
(ASTM A370-10)

4" Straight, P/N 100241

Dimensions of Specimen (in.)	1	2
Width	0.206	0.208
Thickness	0.157	0.158
Area (in ²)	0.0794	0.0803
Tensile strength (psi)	62500	64600
Yield strength 0.2% Offset (psi)	21500	21700
Yield strength 0.2% E.U.L. (psi)	21600	21700
Elongation in 2.0" Gage (%)	20-12	22-12

This testing was completed on December 17, 2013 and performed in accordance with the customer's authorization.

Submitted by:

Redacted

Quality Manager

yy

Appendix B

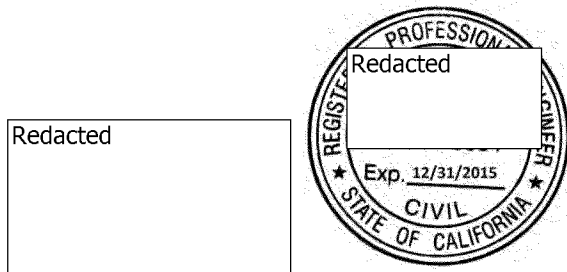
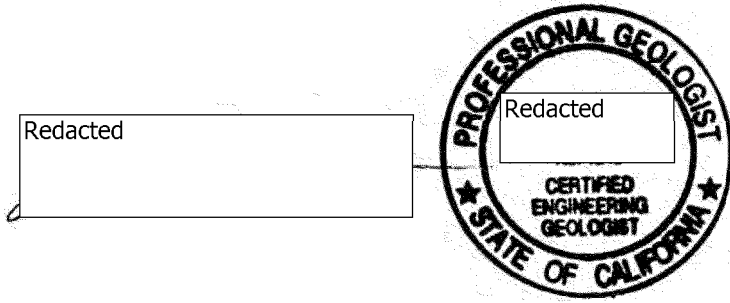
Geotechnical Scope of Work and Signature Page

Geotechnical Scope of Work and Signature Page

Exponent completed the following tasks for the external forces analysis:

1. Performed reconnaissance visits to the release site and nearby areas along the creeping trace of the Hayward Fault.
2. Researched and compiled data on the Hayward Fault and landslides in the vicinity of the release. This task included review of geologic maps, fault maps, landslide maps, historic topographic maps, and historic stereoscopic aerial photographs.
3. Researched and compiled data from long-term fault-creep monitoring in the vicinity of the release by the U.S. Geological Survey (USGS) and San Francisco State University.
4. Reviewed information on water pipe failures in the vicinity of the release provided orally by East Bay Municipal Utility District (EBMUD) to PG&E and, subsequently, to Exponent.
5. Researched and compiled information from records pertaining to fault creep and landsliding at the City of Oakland Building Services Division. This task included geotechnical (soil) reports, geologic reports, selected residential permit files, and City sewer maps.
6. Analyzed the information obtained from Tasks 1 through 5.
7. Observed excavation by PG&E during repair of gas leaks on [Redacted]
[Redacted]
[Redacted] during the period of December 17, 2013 through January 3, 2014.
8. Discussed initial findings with PG&E staff.
9. Prepared this report.

The geologic and geotechnical portions of this report, including the main text as well as Appendices B, C and D, were prepared by the following professionals:



Appendix C

Physical Setting

General Topographic, Drainage and Geologic Setting

Topography and Drainage

[Redacted] follows a nearly level route in the valley of northwest-flowing [Redacted] [Redacted] as shown in Figure C-1. The Site is located at an elevation of approximately 140 feet at the mouth of a [Redacted] that was crossed by [Redacted] and later partially filled for construction of [Redacted] between July 1959 and July 1963.²²

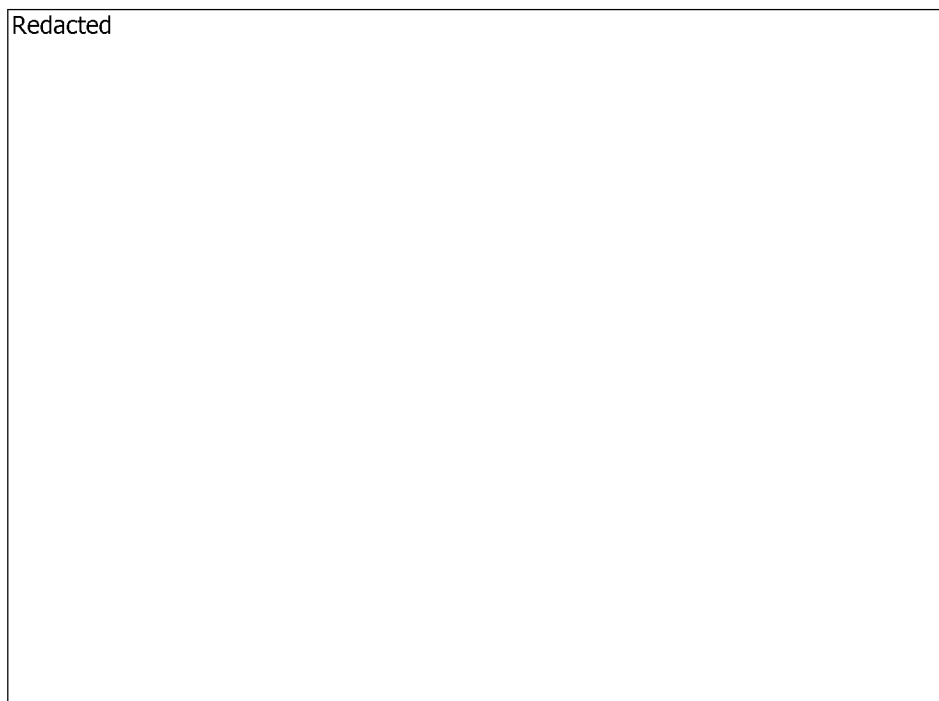


Figure C-1. Topographic location map. Source: USGS, 2012, Oakland East Quadrangle, California, 7.5-minute series, scale 1:24, 000, contour interval 20 feet.

[Redacted] is shown on aerial photographs taken in 1946²³ and on the 1947 topographic map shown in Figure C-2. Figure C-3 shows the topography after construction of [Redacted] [Redacted] and before construction of [Redacted]. The tributary stream is shown flowing from east to west, making a sharp northward bend just east of [Redacted] and entering a culvert beneath [Redacted].

²² Pacific Aerial Surveys (now Photo Science) aerial photographs taken July 8, 1959 (Frames AV-337-09-38 & 39) and July 25, 1963 (Frames AV-550-10-22 & 23).

²³ USGS aerial photograph taken July 29, 1946 (Frame GS-CP 2-38).

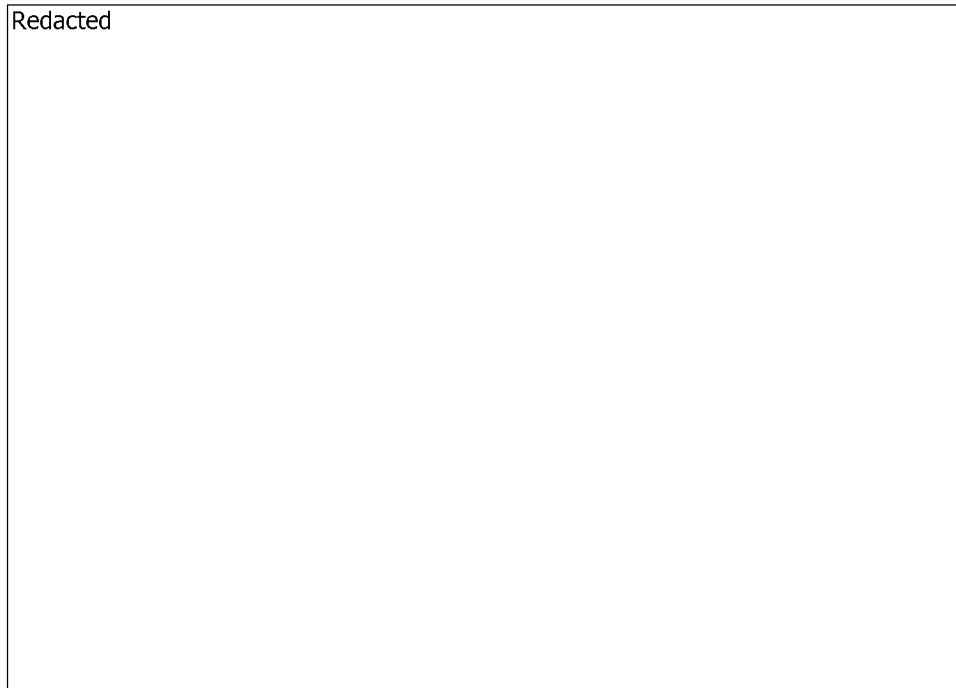


Figure C-2. 1947 topographic map. Redacted is red and white. Source: USGS, 1947, Oakland East Quadrangle, California, 7.5-minute series, scale 1:24, 000, contour interval 20 feet.

Redacted

Figure C-3. Detailed topographic map of Site vicinity with stream channels colored blue (Note: Shows proposed widening of northwestern portion of [Redacted] not implemented). Source: City of Oakland map excerpt, title unknown, date unknown, from Building Services Division Land Stability File 92 L/4, "Grading, 8467 & 8474 [Redacted] 1 of 2."

Geologic Setting

The Site is mapped as being underlain by "undivided surficial deposits,"²⁴ likely stream deposits consisting of gravel, sand, silt, and clay, as shown on the geologic map in Figure C-4. Fill soil placed for construction of [Redacted] across the stream culvert may overlie the native soils at the Site. The adjacent hills are underlain by bedrock and older alluvium,²⁵ which includes older, weakly consolidated stream deposits.

The thick black lines on the geologic map are faults, most of which are part of the active Hayward Fault Zone.

²⁴ Graymer, R.W., Jones, D.L., and Brabb, E.E., 1996, Preliminary geologic map emphasizing bedrock formations in Alameda County, California; a digital database: USGS Open-File Report 96-252, available at <http://pubs.usgs.gov/of/1996/of96-252/>.

²⁵ Ibid.

Redacted

Figure C-4. Geologic map. Pale yellow indicates Qu - undivided surficial deposits; Dark yellow: Qoa - older alluvial deposits; Green: KJk – Knoxville Formation shale and sandstone; Pink: Jsv – Keratophyre and quartz keratophyre (Volcanics), Purple: Jgb – Gabbro; Brown: Jpb – Pillow basalt. Thick black lines indicate faults. Numbers indicate inclinations of faults and bedding planes (90 = vertical). Reference: Graymer, R.W., Jones, D.L., and Brabb, E.E., 1996, Preliminary geologic map emphasizing bedrock formations in Alameda County, California; a digital database: USGS Open-File Report 96–252, available at <http://pubs.usgs.gov/of/1996/of96-252/>.

Appendix D

Creep Monitoring

Creep Monitoring

Creep Monitoring Stations

Figure D-1 shows the location of a creep monitoring station (alinement array) next to Interstate Highway 580. This station (Redacted Station) is located approximately 3,000 feet southeast of the site. This station is currently being monitored annually by San Francisco State University with theodolite surveys of the alinement array. The alinement array at the Redacted Station includes two monuments on opposite sides of the Hayward Fault. The monitoring monuments are 123.80 meters apart.²⁶

²⁶ McFarland, F. S., Lienkaemper, J. J. and Caskey, S. J. (2009, revised 2013). Data from Theodolite Measurements of Creep Rates on San Francisco Bay Region Faults, California, 1979-2012. USGS Open-File Report 2009-1119, v. 1.4. <http://pubs.usgs.gov/of/2009/1119/>.

Redacted

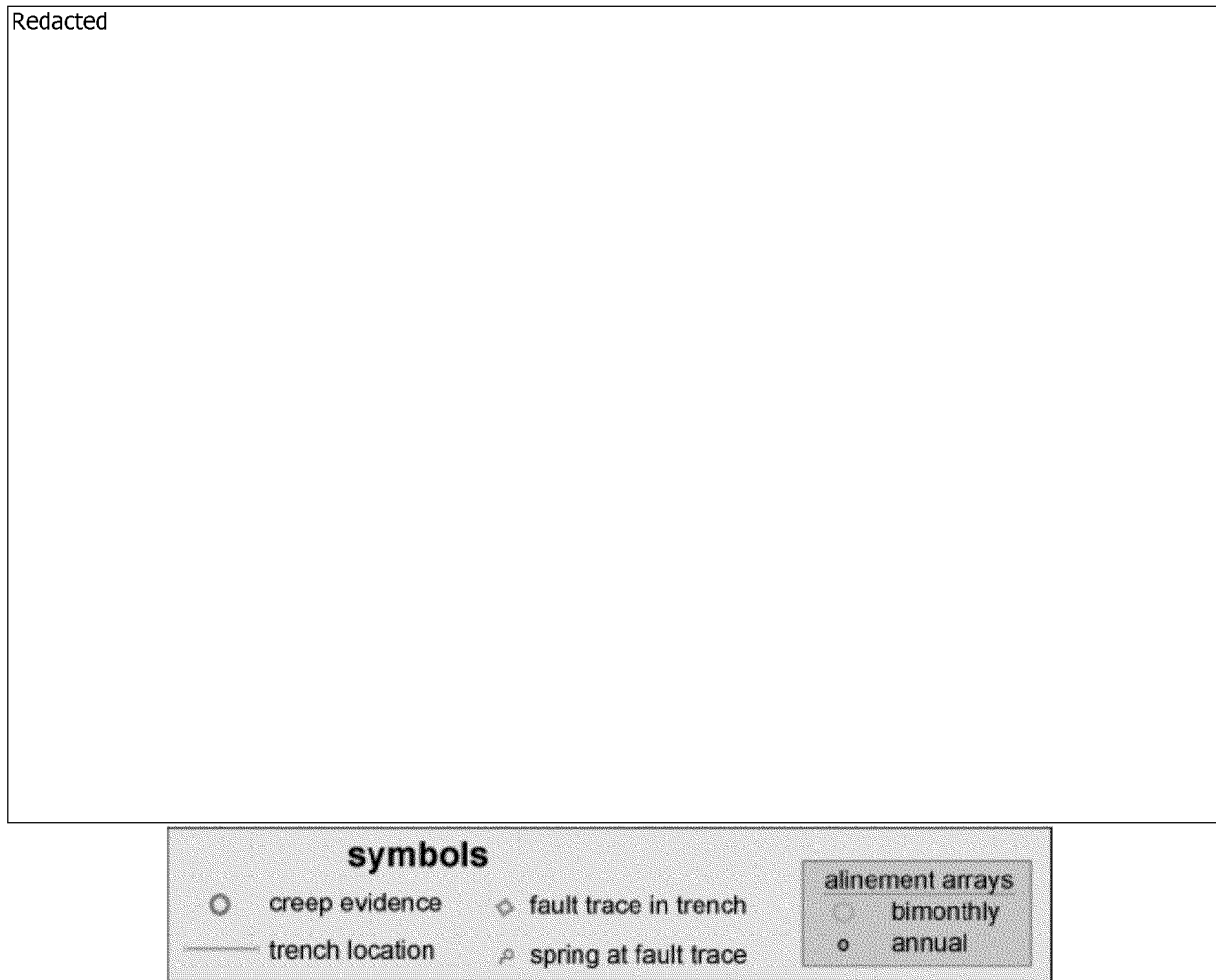


Figure D-1. Map showing recently active trace of Hayward Fault in vicinity of Site. Sources: Lienkaemper, J.J., 2006, revised 2008, Digital database of recently active traces of the Hayward Fault, California: USGS DS-177, <http://pubs.usgs.gov/ds/2006/177/> overlain on 2012 Google Earth air photo.

The USGS also monitors creep rates in the vicinity of the site, at the [Redacted] Station. This station is located approximately 3,900 feet southeast of the site (i.e., approximately 900 feet southeast of the [Redacted] Station). The [Redacted] Station is currently being monitored every 10 minutes by an installed creepmeter. According to the USGS, “Creepmeters consist of two piers separated by about 30 meters and connected by an invar wire. At the [Redacted], the main fault trace lies between the two piers. There is an invar wire oriented roughly a 30 degree angle from the local trace of the fault. A displacement transducer (LVDT) measures the change in length of the wire (or the change in distance between the piers).”²⁷ Figure D-2 shows a schematic of the creepmeter installation at the [Redacted] Station.

²⁷ <http://earthquake.usgs.gov/monitoring/deformation/data/download/table.php>.

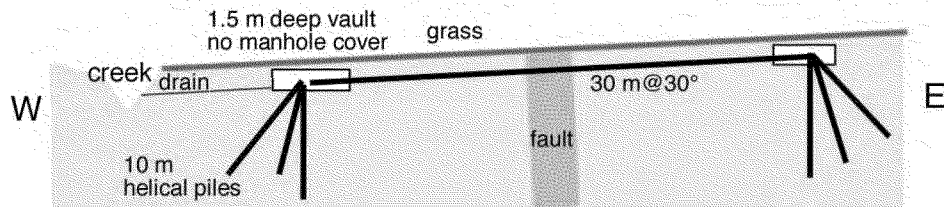
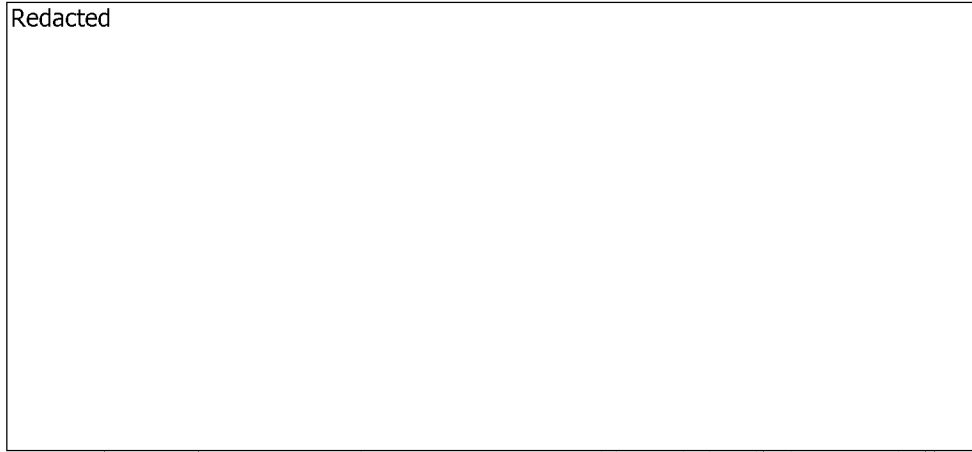


Figure D-2. Site map and cross-section for the [Redacted] Station.
Source: Bilham, Roger. (2007?)²⁸

As will be discussed in more detail later, the average creep rate measured at these two stations ([Redacted]) is approximately the same (Average creep rate = total slip/total time \approx 3.2 mm/yr for [Redacted] and 3.3 mm/yr for [Redacted]).²⁹ This indicates that in the vicinity of the Site, the width of the fault-creep deformation zone is 30 meters or less. This is consistent with conclusions from Lienkaemper (2006, revised 2008), who noted that “detailed mapping and surveying of creep evidence show that the deformation zone of the main creeping trace is as much as 20-m wide.”³⁰

²⁸ Bilham, Roger. (2007?). "Continued Measurement of Fault Creep in the San Francisco Bay Area, and Continued Measurement of Creep and Long-Baseline Deformation in Southern and Northern California." USGS Award 04HQAG0008, Final Technical Report.



Creep Data

For the [Redacted] McFarland et al. (2009, revised 2013)³¹ published creep data that have been recorded since 1989. For the [Redacted] the USGS published creep data that have been recorded since 1996. Figure D-3 shows the available data for these two stations.

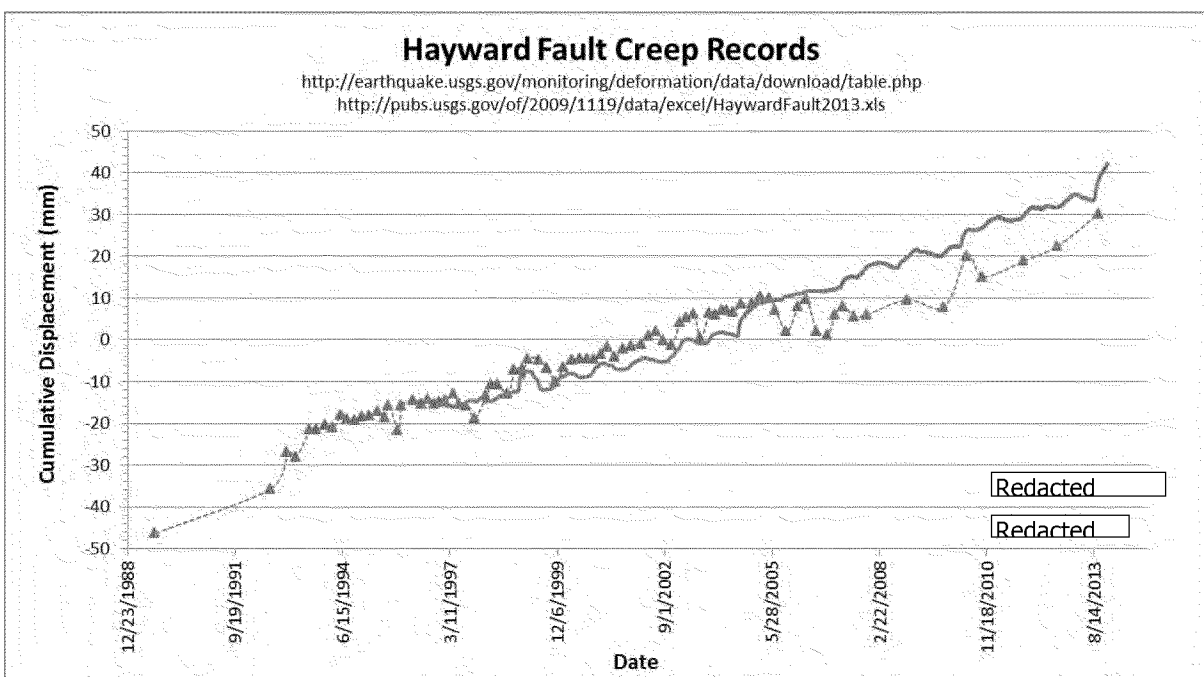


Figure D-3. Hayward Fault creep records in the vicinity of [Redacted] (for available record interval). [Redacted]

As previously noted, at the [Redacted] Station a total displacement of over 76 mm has been measured since 1989, for an average creep rate of 3.2 mm/yr. At the [Redacted] Station a total displacement of over 57 mm has been measured since 1996, for an average creep rate of 3.3 mm/yr.

Figure D-4 shows the 2012 and 2013 portion of the data presented in Figure D-3. The figure shows an acceleration of creep movement measured at the [Redacted] station starting in approximately August 2013. The timing of the gas release event may be related to this acceleration of creep movement.

³¹ McFarland, F. S., Lienkaemper, J. J. and Caskey, S. J. (2009, revised 2013). Data from Theodolite Measurements of Creep Rates on San Francisco Bay Region Faults, California, 1979-2012. USGS Open-File Report 2009-1119, v. 1.4.

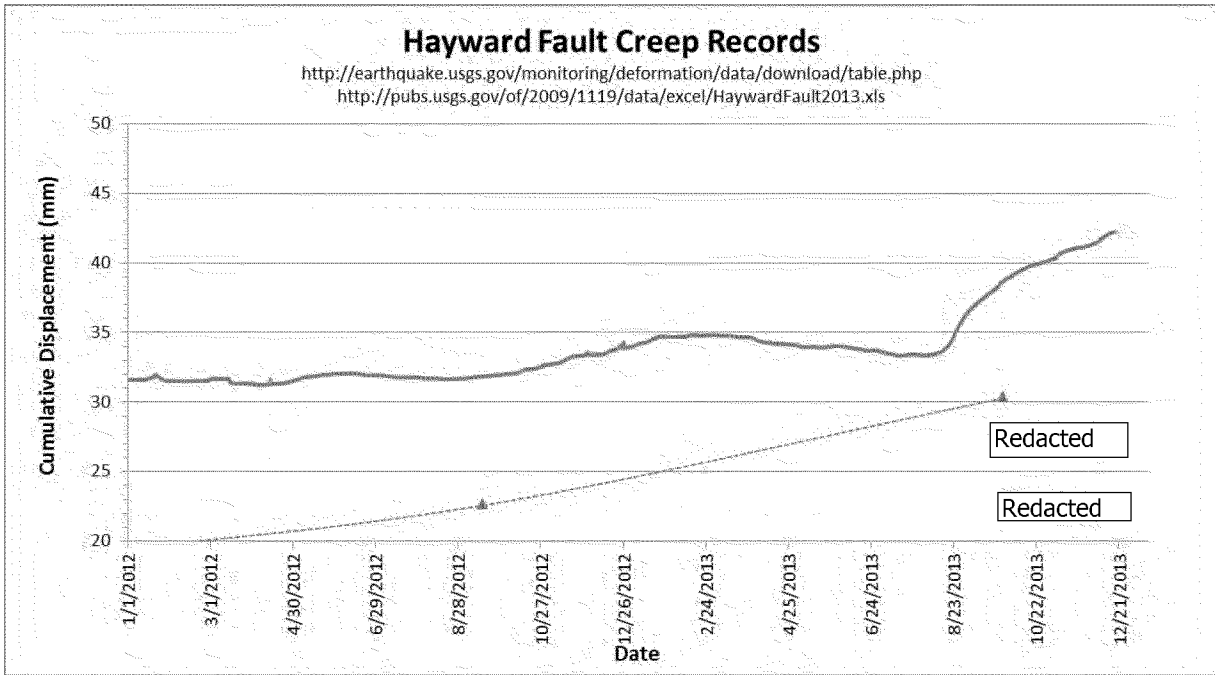


Figure D-4. Hayward Fault creep records in the vicinity of [Redacted] (for 2012 and 2013). [Redacted]